Sanz-Robinson, J., Williams-Jones, A.E., 2020.
The solubility of Nickel (Ni) in crude oil at 150, 200 and 250 °C
and its application to ore genesis. Chemical Geology, 533: 119443.

The solubility of Nickel (Ni) in Crude Oil at 150, 200 and 250°C and its Application to Ore Genesis

J. Sanz-Robinson*[a] and A.E. Williams-Jones[a]

[a] Department of Earth and Planetary Sciences, McGill University, 3450 University Street, Montreal, QC, H3A 0E8, Canada.

Abstract

The very low solubility of Ni in saline brines and the correspondingly high concentration of Ni in some crude oils raises the possibility that liquid hydrocarbons may be the ore fluids for black-shale-hosted Ni deposits. To test the feasibility of this hypothesis, Ni wires were reacted with three crude oils of differing composition at 150, 200 and 250°C for up to 30 days, and the concentration of Ni in the oil determined. At 150°C, Ni concentrations in the three oils remained relatively low. Above 200°C, however, Ni concentrations were elevated and correlated positively with the thiol content of the oil. Our most thiol-rich oil dissolved 217 ± 40.4 ppm Ni after 30 days at 250°C. X-ray photoelectron spectroscopic (XPS) analyses performed on the residual oil coating the Ni wires after reaction independently corroborate the conclusion that Ni has a strong chemical affinity for thiols in crude oil. Furthermore, in crude oils with no thiols, the Ni reacted with other sulfur compounds (potentially sulfonic acids) in oil to form thiols. Significantly, our XPS analyses show that iron (Fe) from the oil was embedded in the Ni wire synchronously with the attachment of thiols. This suggests that Fe has an affinity for Ni and that the thiolation of Ni by crude oil may depend on the availability of Fe in the oil. In addition to thiols, porphyrins also

likely play an important role in the dissolution of Ni, as shown by the fact that the oil in which Ni was most soluble has a high nitrogen content, whereas in the other oil, which is characterized by a high thiol content, the Ni solubility was relatively low and the nitrogen content of this oil was below the detection limit. Immature biodegraded oils that are sourced from carbonate rocks generally tend to be enriched in asphaltenes, Ni and sulfur. Nevertheless, some mature oils acquire anomalously large thiol contents through Thermochemical Sulfate Reduction (TSR), a high temperature (100 to 140°C) reaction occurring commonly in carbonate reservoirs, which involves the abiotic reduction of sulfate minerals at the expense of oil or bitumen. Thus, given the affinity of Ni for thiols, large volumes of Ni-poor oil can potentially be altered by TSR to produce smaller volumes of residual oil enriched in thiols and Ni.

1. Introduction

Nickel (Ni) commonly forms organometallic complexes with nitrogen-bearing ligands such as tetrapyrroles and sulfur-bearing ligands, e.g., thiols in living organisms, organic sediments, oil and bitumen (Parnell, 1988). For example, the Ni-F_{430} co-enzymes present in methanogens are Ni-tetrapyrrole complexes (Diekert et al., 1981) and the most common form of hydrogenase enzyme present in anaerobic microorganisms consists of organometallic iron-nickel (Fe–Ni) complexes bound together by cysteinyl thiolate ligands (Ohki and Tatsumi, 2011). Nickel and sulfur are also enriched in the asphaltene phase in bitumen and petroleum (Parnell, 1988; Yu et al., 2015), which is composed of large (500-1000 Da) heterocyclic molecules such as tetrapyrroles (Groenzin and Mullins, 1999).

Occurrences of Ni-rich bitumen veins in Peru, Argentina and Venezuela and high levels of Ni and Vanadium (V) in Venezuelan oils and coals, according to Kapo (1978), may be genetically related to Ni and V ore deposits in the watershed. Moreover, several ore grade Ni deposits elsewhere, notably the Zunyi Deposit in Southern China, the Nick and related prospects in the Yukon, Canada and the Talvivaara deposit in Finland, are hosted in sediments, which may have been infiltrated by petroleum. The relationship between petroleum and anomalous Ni enrichment in organic-rich sedimentary rocks is intriguing.

The Zunyi deposit in Southern China and the prospects of Yukon, Canada, are metalliferous black shales that share many similarities, most notably that the ore horizon in both localities consists of a thin (between 10 and 30 cm thick), stratiform layer of sulfide minerals with weight percent enrichments of Ni (Jowitt and Keays, 2011). Both deposits also display signs of having interacted with liquid hydrocarbons. For example, evidence of migrabitumen in the Zunyi deposit may indicate that the latter was brecciated during late diagenesis, allowing it to act as an "oil collector" (Kříbek et al., 2007). Similarly, large, bituminous veins in the Nick Prospect in Yukon Canada, have been interpreted as evidence for the passage of hydrocarbon-rich fluids through the mineralized horizon (Hulbert et al., 1992, Henderson et. al., 2019). Unlike the aforementioned metalliferous shales, the Talvivaara deposit, located in the central part of the Fennoscandian Shield, has a considerably thicker ore horizon (up to 330m thick) and contains 300 million metric tons (Mt) of ore averaging 0.26 wt,% Ni, 0.14 wt.% Cu, and 0.53 wt.% Zn with minor concentrations (10-30 ppm) of uranium (U) (Loukola-Ruskeeniemi and Heino, 1996; Lecomte et al, 2014). The presence of bitumen rims on uraninite crystals from the Talvivaara deposit suggests a close association with liquid hydrocarbons (Lecomte et al, 2014).

As discussed above, liquid hydrocarbons may have interacted with the black shales hosting several Ni-rich deposits. Here, we examine the physical and compositional parameters that control Ni solubility in oil to determine the potential of crude oil to act as a Ni ore fluid. We do so, using the results of experiments designed to determine the solubility of Ni wire in crude oil at temperatures of 150, 200 and 250 °C, a range consistent with conclusions from pyrolysis experiments (Price and Wenger, 1992) and studies of liquid hydrocarbons entrapped in black smokers (Peter and Scott, 1988) that liquid hydrocarbons remain stable to temperatures above 300°C for protracted periods of time. Finally, we use the results of this study to examine the hypothesis that Ni-enriched deposits in sedimentary basins may be the products of Ni-rich oils.

2. Materials and Methods

2.1 Crude Oil Characterization

The crude oils selected for this investigation and compositional data for them were provided by Statoil Canada. These oils have markedly different compositions and physical properties (Table 1). This is important for isolating the compositional parameters, which affect the dissolution of Ni in crude oil. The selected oils vary in specific gravity from 0.90 to 0.94 and have varying asphaltene contents. The asphaltene phase of petroleum is composed of large heterocyclic molecules and is particularly important to the context of this investigation given that Ni is commonly concentrated in the asphaltene fraction of petroleum (Parnell, 1988; Groenzin and Mullins, 1999). In our oils, the asphaltene content ranges from below 0.3 wt.% up to 1.6 wt. %. The selected oils also differ in their Total Acid Number (TAN), a measure of their carboxylic

acid content (Seifert, 1975) and contain sulfur compounds (e.g., thiols, thiophenes, benzothiophenes, dibenzothiophenes and benzonaphtothiophenes) in varying abundances. Certain sulfur species, such as thiols, are recognized for their ability to form organometallic complexes (Lewan, 1984; Giordano, 1994; Speight, 2001). Finally, the nitrogen content of our oils varies between 0.2 and 0.44 wt. %. Nitrogen is an important compositional parameter as certain nitrogen bearing species in petroleum, such as porphyrins, are known for their ability to bind stably to Ni (Barwise, 1990). Compounds, such as pyrroles, pyridines and saturated amines, also contribute to the nitrogen budget of crude oil (Mitra-Kirtley et. al., 1993).

Table 1. The composition and properties of the three crude oils, A, B and C, employed in our experiments.

Parameters	Oil A	Oil B	Oil C
API Gravity	26.6	25	19
Specific Gravity	0.895	0.904	0.94
Sulfur (wt.%)	0.84	0.52	0.82
Thiols/sulfides (ppm)	44	0	52
Thiophenes/Disulfudes (ppm)	1400	37	1050
Benzothiophenes (ppm)	3890	1880	3160
Dibenzothiophenes (ppm)	2580	2740	2020
Benzonaphtothiophenes (ppm)	490	549	109
Nitrogen (wt.%)	---	0.2	0.44
TAN (mgKOH/g)	0.2	2.9	2.3
Paraffins (wt.%)	---	37	19

Naphthenes (wt.%)	---	49	65
Aromatics (wt.%)	---	13	15
Asphaltenes (wt.%)	1.6	0.3	1.4
Background Ni (ppm)	5.59	4.05	6.22
Background Fe (ppm)	0.343	8.71	16.5

2.2 Solubility and speciation of Nickel in liquid hydrocarbons

In order to determine the solubility of elemental Ni in crude oil, Ni (0) wires (≥99.9%) from Sigma-Aldrich® were reacted in crude oils A, B and C for varying lengths of time following the procedure established in Sanz-Robinson and Williams-Jones, (2019). This involved reacting a Ni wire in oil inside a sealed quartz tube. Prior to being used, the quartz tubes were cleaned with trace-metal grade nitric acid (~75% HNO_3) for 24 hours, neutralized with Milli-Q™ water and dried at 100 °C for 2 hours. A Ni wire was placed in the reaction tube and an aliquot of crude oil (~0.5mL) was pipetted into the tube. The loaded reactors were then placed in a Thermo Scientific™ Thermolyne™ tabletop muffle furnace oven that had been preheated to the desired temperature. This procedure was repeated for varying periods of time (5, 10, 15 and 30 days) at 150°C, 200°C and 250°C.

After each experiment, the reaction vessel was removed from the furnace and quenched immediately in a beaker of tap-water at room temperature. The tubes were then opened using a file and the Ni wire was removed. The reacted oil was combusted in a muffle furnace at 550°C for 24 h and the resulting char was digested in a solution of 0.25 ml of 75% Optima™ grade HNO_3, 0.5 ml of Optima™ grade H_2O_2 and 0.25 ml of Optima™ grade HCl for a further 24h in

order to oxidize the remaining char and dissolve the metal. The leaching solution was diluted with a solution of 2% Optima™ grade HNO_3 and analysed with the Thermo Scientific™ iCAP™ Q inductively coupled plasma mass spectrometer (ICPMS) in the ICP Laboratory of the Department of Earth and Planetary Sciences at McGill University. Yttrium was used as an internal standard for the ICPMS analyses.

The reacted Ni wires were rinsed in toluene (≥99.5%) purchased from Fischer Scientific, vacuum-dried for 24 h and analyzed by X-ray photoelectron spectroscopy (XPS) to determine the composition of the residual oil bound to the wire. For the purpose of comparison, the procedure was repeated for Ni wires that had been immersed in the three oils at ambient temperature. The analyses were conducted with a Thermo Scientific Kα™ spectrometer at the McGill Institute for Advanced Materials (MIAM). Analyses were performed using Al Kα™ radiation (1486 eV) and an X-ray spot size of 100 μm, and scans were made with a pass energy of 50 eV and a resolution of 0.1 eV. The C1S, C-C peak at 284.8eV was used as a charge-reference peak to ensure adequate peak alignment. The Thermo Scientific Kα™ spectrometer etching function was used to progressively etch the Ni wire, thereby removing weakly bound surficial ligands and exposing deeply embedded ligands with a strong chemical affinity for Ni.

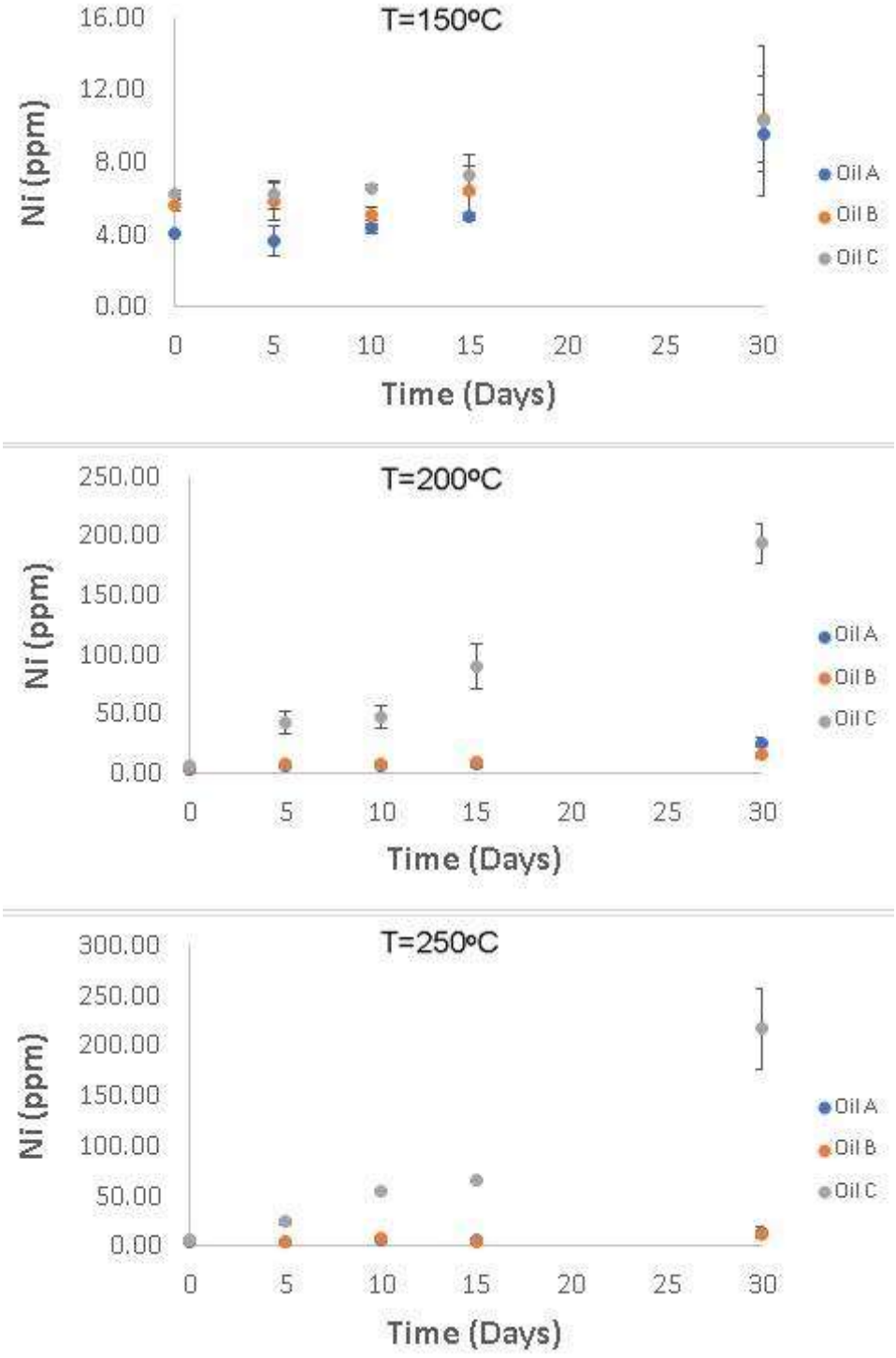

Figure 1. The concentration of Ni (3 S.D.) in crude oils A, B and C at 150, 200 and 250 ˚C as a function of the duration of the experiments. The vertical lines are error bars indicating the experimental uncertainty.

3. Results

3.1 Nickel solubility

Nickel wires were reacted with crude oils A, B and C for 5, 10, 15 and 30 days at 150, 200 and 250°C in order to establish the steady state Ni concentrations. Three experiments were performed for each oil at each temperature and for each duration, and the average temperature and standard deviation for each set of experiments determined. As the Ni concentrations increased with time and were highest after 30 days (Fig. 1), we consider the average concentrations obtained for this duration to represent the minimum solubility of Ni in the corresponding oils (Table 2).

Nickel concentrations in the crude oil were relatively low at 150°C, with all oils dissolving approximately 10 ppm Ni. Progressive heating, however, resulted in a significantly higher solubility of Ni in Oil C (Figure 1) relative to the other oils; Oil C dissolved 194 ppm Ni at 200°C and 217 ppm Ni at 250°C, whereas Oil A dissolved 25.7 and 13.8 ppm at these temperatures and Oil B dissolved 15.6 and 12.3 ppm, respectively (Table 2). Oil C has the highest thiol and iron content of the three oils considered, followed by Oil A, which dissolved the second largest amount of Ni, albeit a considerably lower amount than Oil C. The asphaltene and sulfur content of Oils A and C are similar, but Oil A has a considerably smaller TAN and Fe content. Oil B dissolved the least Ni of the three crude oils. It has the largest TAN number but a much smaller asphaltene fraction than Oils A and B, has a moderate Fe content and contains no detectable thiols.

Table 2. Results of experiments designed to determine the solubility of Ni in crude oils A, B and C at 150, 200 and 250 ˚C. The Ni concentration at 25˚C is the background concentration in the unreacted oil.

	Oil A			Oil B			Oil C		
Temp.	**n***	**Ni (ppm)**	**Error (ppm)**	**n***	**Ni (ppm)**	**Error (ppm)**	**n***	**Ni (ppm)**	**Error (ppm)**
25 ˚C	3	5.59	0.32	3	4.05	0.03	3	6.22	0.220
150 ˚C	3	9.62	2.15	3	10.40	2.39	2	10.30	4.14
200 ˚C	3	25.7	4.08	3	15.60	2.54	2	194.00	17.20
250 ˚C	3	13.80	6.36	3	12.30	1.63	3	217.00	40.40

n* is the number of experiments conducted

3.2 Results of X-ray Photoelectron Spectroscopy Analyses

An XPS scan (Figure 2) performed on the residue of oil on a Ni wire after reaction with Oil C (Ni solubility is highest in this oil) at 200°C, showed that the wire is coated mainly with carbon (C), sulfur (S) and oxygen (O). The wire was etched with an argon ion beam to remove weakly bound surficial ligands. After etching, the amounts of C and O decreased, whereas the relative proportions of Ni and S increased. This shows that Ni has a strong chemical affinity for S in crude oil. An enlargement of the S peak (Figure 3a) shows that it is centered at a binding energy of ~163 eV, which corresponds to the thiol functional group (Castner et. al., 1996). This indicates that S, and more specifically thiols in Oil C, have a strong chemical affinity for Ni. The XPS scan of the wire that had been immersed in Oil C at ambient temperature also yielded a spectrum with a thiol peak (~ 163 eV) but, in addition, the spectrum contained a peak at ~168 eV corresponding to an oxidized sulfur species, possibly a sulfonic acid (Figure 3b). Similar results

were obtained for Oil A after reaction at 200 °C and for ambient temperature, respectively (Appendix, Figure A1a and b).

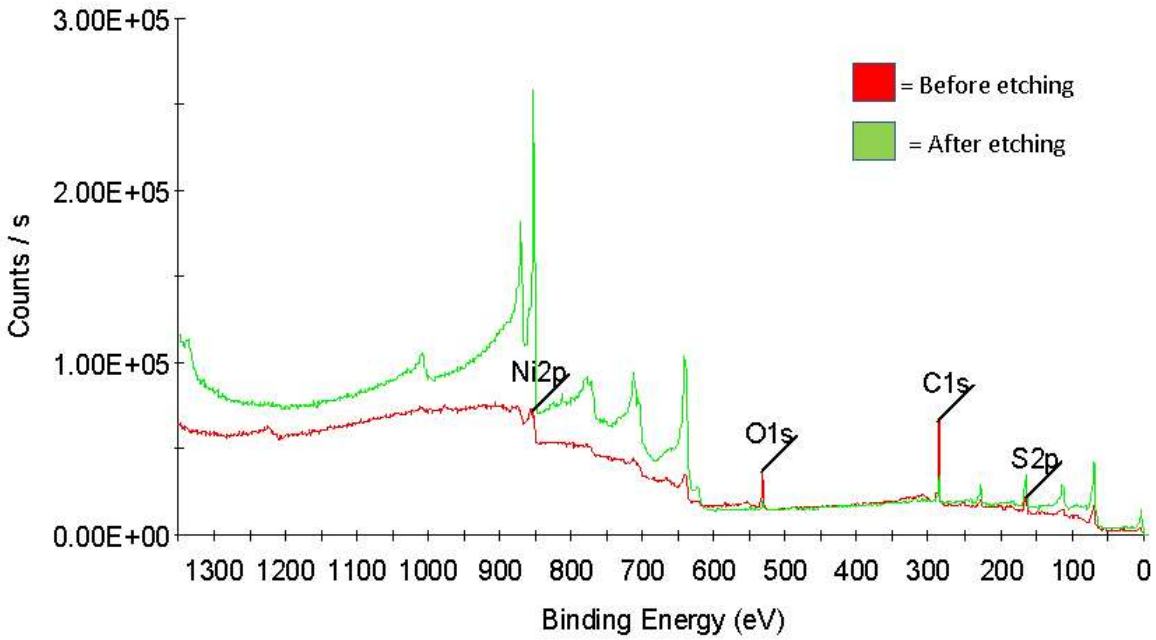

Figure 2. A XPS spectrum identifying the major elements bound to the Ni wire after reaction with Oil C at 200˚C. The relative abundances of these elements changed as the wire was progressively etched. Peak binding energies for the different elements are as follows: S 2p =163eV, C 1S= 285eV, O 1S = 532eV and Ni 2p = 853eV. The peaks between 650eV and 750eV that appear after etching are Ni Auger Lines, resulting from the relaxation of core Ni electrons (Wagner, 1972, Potočnik et. al., 2016)

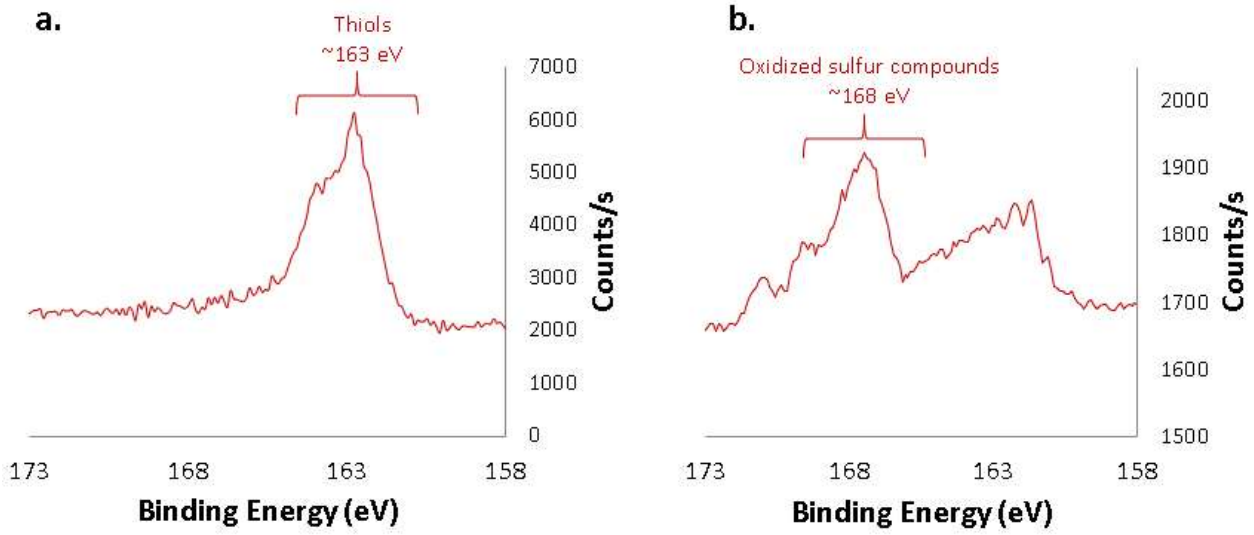

Figure 3. An XPS spectrum illustrating the sulfur speciation of residual oil on a nickel wire after reaction with Oil C at a) 200°C and b) ambient temperature. The sulfur 2p peak centered at a binding energy of 163eV corresponds to the thiol functional group whereas the sulfur 2p peak centered at 168eV corresponds to oxidized sulfur compounds.

Predictably, and in contrast to the spectra for Oils A and C at ambient temperature, the Ni wire spectrum for Oil B (which does not contain detectable thiols) at this temperature did not contain a thiol peak (~ 163 eV), although, like the other oils it did contain a peak for an oxidized sulfur species (~ 168eV) (Figure 4a). Somewhat unexpectedly, however, the spectrum obtained for Ni wire after reaction with Oil B at 200 °C contained a thiol peak (~ 163 eV) (Figure 4b). We interpret this finding to indicate that the Ni wire catalytically reduced oxidized forms of sulfur in the oil like sulfonic acids to thiols (Kelemen et. al., 1990).

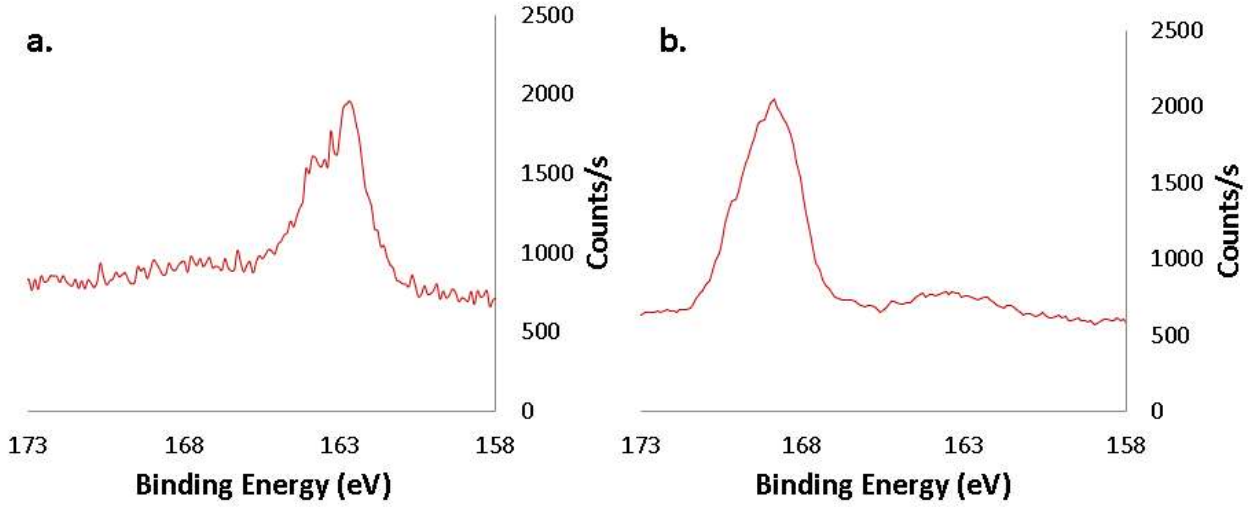

Figure 4. An XPS spectrum illustrating the sulfur speciation of residual oil on a nickel wire after reaction with Oil B at a) 200°C and b) ambient temperature.

The thiolation of the Ni wires and the dissolution of Ni in Oil B and C also coincided with the incorporation of iron (Fe) from the oil into the Ni wires, albeit in trace amounts (< 1 atom % of the Ni wire surface). This is evident in Figure 5 by the presence of an Fe doublet with peaks at 706 and 714 eV, which appeared after etching the Ni wire. Thus, Fe also displays a strong chemical affinity for Ni and may participate in the redox reactions that occur between the Ni wire and sulfur compounds in the oil.

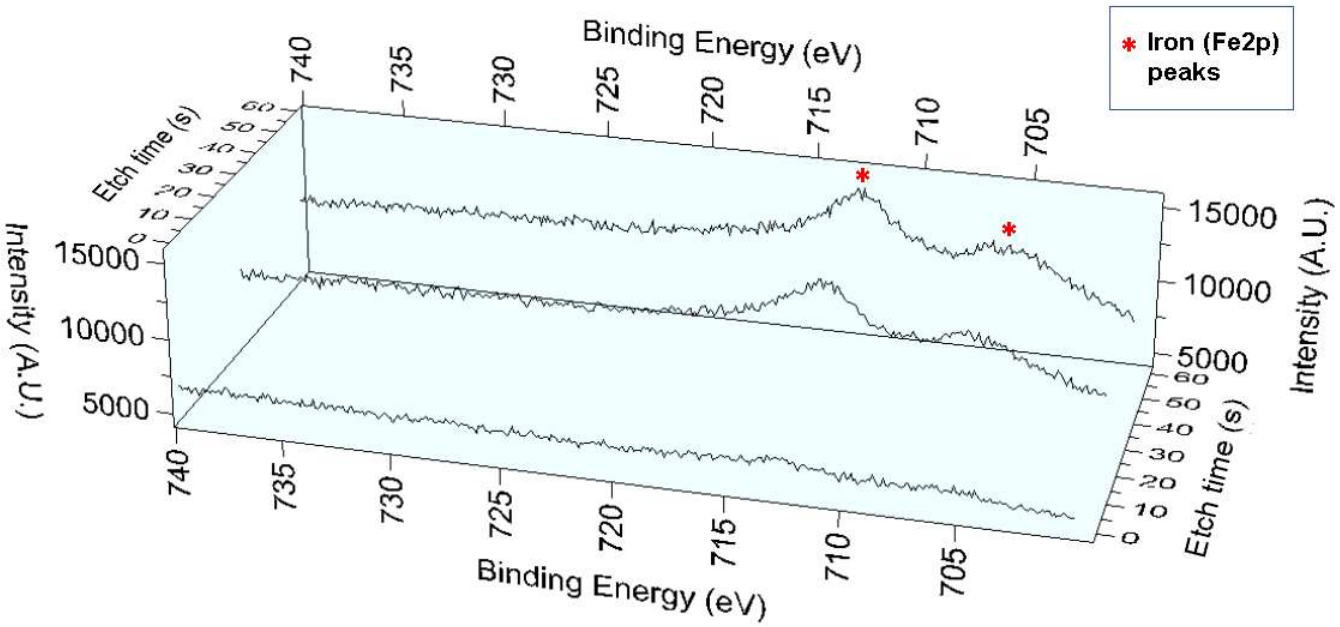

Figure 5. An XPS spectrum of the nickel wire after reaction with Oil C at 200°C. Progressive etching revealed the presence of trace amounts of iron.

4. Discussion

4.1 Nickel solubility and speciation in liquid hydrocarbons as a function of petroleum composition.

In addition to testing the hypothesis that crude oils can dissolve significant amounts of Ni, the experiments described above were conducted to identify the compositional factors controlling the dissolution of Ni in liquid hydrocarbons. At 200°C and higher temperature, Oil C has a much greater capacity to dissolve Ni than the other crude oils (Table 2), which in part reflects the fact that it has the highest thiol content of the three oils. This high thiol content, however, does not explain the observation that the solubility of Ni in Oil C is nearly eight times higher than that of Oil A, whereas the thiol content of the latter oil is roughly 80% of that of Oil C (Table 1 and 2). The high Ni content of Oil C relative to Oil A also cannot be attributed to differences in the

asphaltene content (Ni, like other metals has been shown to concentrate in the asphaltene fraction of crude oils; Marcano et. al., 2011), because the asphaltene contents of the two oils are very similar and, indeed, the asphaltene content of Oil A is slightly higher than that of Oil C (1.6 versus 1.4 wt.%). The two oils do, however, differ in their nitrogen contents and TAN values. Oil C has the highest nitrogen content of the three oils (0.44 wt.%), whereas nitrogen was not detected in Oil A (Table 2). This may indicate that a significant proportion of the Ni in Oil C dissolved as porphyrin species, an observation that has been made for other crude oils (Ali et. al., 1993). As the TAN value of Oil C is very much higher than that of Oil A (2.3 versus 0.2) and this value is an indicator of the carboxylic acid content, it is also possible that the binding of Ni by thiols in Oil C was greatly enhanced by the much higher acidity of this oil (Wenger et. al., 2002. Clegg and Henderson, 2002). Significantly, Oil B has the highest TAN value (2.9 wt.%), which may help explain the fact that it dissolved some Ni (15.6 ppm at 200 °C), despite being thiol-free initially (thiols formed during the experiments due to Ni catalysed reduction of oxidized sulfur species; see above). Given that Oil A contains some nitrogen (0.2 wt.%), it is likewise possible that Ni in this oil was dissolved in large part as porphyrin species.

The thiolation of Ni may also involve Fe, which is the only other chemical component in the oil, aside from thiols that showed an affinity for the Ni wire. The intimate association of Ni, Fe and thiols on the wire surface indicates that Fe may be involved in the redox processes that helped dissolve Ni into the oil. Oil C has the highest Fe content of all the oils and displays a strong Fe peak upon etching, whereas Oil A has the lowest Fe content and shows little evidence of complexing with Fe. This also may help explain why these two oils dissolve very different amounts of Ni. In principle, Fe could have enhanced the dissolution of Ni by forming Ni-Fe-

sulfur clusters, i.e., stable complexes of Fe and Ni bound together by thiolate ligands that are ubiquitous in nature (Ragsdale, 2009).

4.2 Geochemical factors affecting oil composition and ore deposit formation

The polar compounds in crude oil (also referred to as NSO compounds) contain one or more heteroatoms of nitrogen(N), sulfur(S) or oxygen(O) and, although they typically compose less than 10 wt% of petroleum, they are considered important ligands for metals in crude oil (Hughley et. al., 2004). With the increasing maturity of oils, their NSO content generally decreases, whereas their gasoline content increases (Meyer, 1989). Thus, Ni transport is favored by immature oils, particularly those that have experienced strong biodegradation, as these oils generally have higher NSO contents than less biodegraded oils of similar maturity (Meyer, 1989; Wenger et. al., 2002; Head et. al., 2003). Biodegraded immature oils are also characterized by high asphaltene contents. Nickel concentrations are highest in immature oils derived from carbonate source rocks with a low clay content and a high reduced sulfur content (this is likely due to Ni complexation by thiols). By comparison, marine and lacustrine shales generate oils with moderate amounts of Ni, and land-plant derived oils contain very little Ni (Meyer, 1989; Barwise, 1990). For example, crude oils generated in carbonate source rocks from the Gulf of Suez and Abu Dhabi have been documented to contain Ni in concentrations, which range from 4 ppm to 148 ppm Ni, whereas oils generated from non-carbonate source-rocks in the North Sea, mainland China, Indonesia and the Gippsland Basin in Australia have Ni concentrations in the 0.13 ppm Ni to 22 ppm Ni range (Barwise, 1990).

As noted above, nickel has an affinity for the asphaltene fraction of crude oil (Sugihara and Bean, 1962; Parnell, 1988; Yu et al., 2015). Indeed, the Boscan Crude oil from Venezuela, which has an asphaltene fraction corresponding to 20 wt% of the oil (Sugihara and Bean, 1962; Fish et al., 1984), contains up to 115 ppm Ni (Sugihara and Bean, 1962). Moreover, 78% of the Ni in this oil is contained within the asphaltene fraction (Fish et al., 1978). The asphaltene phase in petroleum is composed of large heterocyclic compounds, such as porphyrins (a form of tetrapyrrole), which are generated from the break-down of kerogen in the source rocks during catagenesis (Orr., 1986). Major precursors for porphyrins in oil are the chlorophylls present in photosynthetic organisms (Hodgson, 1973). In the Boscan Crude oil, 36 wt% of the metals in the asphaltene fraction are bound to porphyrins (Sugihara and Bean, 1962). Little is known, however, about the other kinds of organometallic complexes that form with Ni in petroleum, which are potentially more abundant than the Ni-porphyrins and may account for up to 50–80% of the metal being complexed in oil (Caumette et. al., 2009).

In addition to its association with porphyrins, Ni possesses a strong chemical affinity for thiols, as has been shown in this study. Despite the decreasing trend in the proportion of NSO compounds with oil maturity, some very mature oils can contain anomalously high concentrations of thiols. These oils are typically sourced from deep, high temperature carbonate reservoirs with high partial pressures of hydrogen sulfide gas. The hydrogen sulfide in these reservoirs is thought to be produced by thermochemical sulfate reduction (TSR) (Ho et al., 1974), a redox reaction between sulfate minerals and organic matter, which involves the high temperature, abiotic reduction of sulfate (see Equation 1 below). The hydrogen sulfide produced by TSR can react with organic compounds in liquid hydrocarbons, leading to the formation of

thiol-enriched oils (Ho et al., 1974; Cai et al., 2003; Wei et al., 2011; Nguyen et al., 2013). Oil C, our most thiol-enriched oil (52 ppm thiol) has a relatively low thiol content compared to crude oils described in the literature, which have undergone TSR. For example, the "Rodney Crude" and the "Light Mixed B.C." oils described by Ho el al. (1974) have thiol contents of 3179 ppm and1310 ppm, respectively, as calculated from their mercaptan numbers (refer to Appendix A for a calculation of the thiol content of the Rodney Crude Oil). Anomalously thiol-rich oils, which have undergone TSR, therefore, may be expected to transport considerably greater concentrations of Ni than Oil C.

Thermochemical sulfate reduction:

$$\text{Hydrocarbons} + SO_4^{2-} \rightarrow \text{Altered hydrocarbons} + \text{bitumen} + H_2S + HCO_3^- + H_2O \quad (1)$$

(Machel, 2001)

Thermochemical sulfate reduction is a common source for the reduced sulfur responsible for the formation of Mississippi Valley Type (MVT) deposits (Machel, 2001) and is interpreted to be the source of reduced sulfur for the sulfide ores in other sediment-hosted deposits, such as the Kuperschiefer deposit in Poland (Bechtel and Püttmann, 1991; Jowett et al., 1991; Sun, 1998; Oszczepalski et al., 2012) and the Ni-rich sulfide ores in the Talvivaara deposit in Finland, which displays mass-anomalous $\Delta^{33}S$ fractionation similar to that of TSR laboratory experiments (Young et. al., 2013). Thus, the genesis of some sediment-hosted sulfide deposits may be related through TSR to the production of a metalliferous, thiol-rich oil.

4.3 Evidence for the involvement of liquid hydrocarbons in the genesis of shale-hosted nickel deposits.

The two currently favored models for the formation of sedimentary Ni-rich deposits are: 1) synsedimentary mineralisation, with the metals being scavenged from seawater by organic matter close to the seawater-sediment interface (Lehman et al., 2007; and 2) exhalative hydrothermal mineralisation, with the metals being deposited from basinal brines as they are discharged into a euxinic, stratified water mass (Jowitt and Keays, 2011). Given that petroleum can dissolve considerable amounts of Ni, a petroleum exhalative (Petrex) model has also been proposed to describe the genesis of certain Ni-rich sedimentary deposits, e.g., the Zunyi deposits in China. In this model, petroleum is discharged into the basin and forms a sea-surface slick. Metals are then deposited as the oil is volatilized, water-washed, oxidized and biodegraded (Emsbo et. al., 2005).

Here, we discuss the evidence for the involvement of liquid hydrocarbons in the genesis of shale-hosted nickel deposits. The principal examples of these deposits are the hyper-enriched black shale (HEBS) deposits in southern China and the Nick Prospect and related prospects in the Yukon, Canada. These deposits comprise thin highly enriched metal-sulfide layers, usually no more than no more that 30 cm thick in southern China and 10 cm thick in the Yukon, with Ni grades of up to 7 wt% and 5.7 wt%, respectively (Jowitt and Keays, 2011; Henderson et al., 2019). They outcrop discontinuously for 2000 km in southern China and > 800 km in the Yukon. Organic particles commonly fill voids and fissures in the mineralized black shale of southern China and most probably represent partly remobilized and solidified products of oil migration

(migrabitumens) (Kříbek et al., 2007). The restriction of migrabitumen to the ores and their absence in the barren shales likely reflect a higher primary porosity of the ore horizon (breccia) compared to the barren shale. Thus, the ore horizon probably played the role of an "oil collector" during late diagenesis and catagenesis (Kříbek et al., 2007). At the Nick prospect, pyrobitumen occurs as centimetre-scale veinlets within the mineralized layer and meter-wide subvertical veins in the shales stratigraphically below this layer. Moreover, pyrobitumen within the mineralized layer contains 1300 ppm Ni on average and elevated concentrations of other metals. and one of the thicker veins below the layer contains 2000 ppm Ni (Henderson et. al, 2019).

It is noteworthy that there are numerous oil and gas fields of Sinian to Cambrian age (Sichuan Basin) in relatively close proximity to some of the HEBS deposits in southern China (EIA 2011; Lan et. al., 2017; Pages et. al., 2018). The gas in these fields is interpreted to have formed through the thermal cracking of petroleum (Hao et. al., 2008; Caineng et. al., 2014; Zou et. al., 2014; Zhu et. al., 2015) and in many cases, there is evidence that there was gas souring from TSR (Cai C. et. al., 2003; Hao et. al., 2008; Zhu et. al., 2015). As crude oil starts to undergo TSR, it becomes oxidized at the expense of aqueous sulfate in the reservoir, which is reduced to hydrogen sulfide gas (Machel, 2001). The residual oil that has undergone TSR is anomalously enriched in thiols (Ho et al., 1974; Cai et al., 2003; Wei et al., 2011; Nguyen et al., 2013), which display a strong affinity for metals like Ni and Pd (Sanz-Robinson et. al., 2019). These residual oils are therefore potentially effective ore fluids for the transport of Ni and Pd and perhaps other noble metals like Pt, Os and Au, all of which share similar electronegativity and therefore, according to hard-soft-acid-base principles are expected to bind to 'soft' ligands like thiols (Pearson, 1963). Furthermore, the oxidation of petroleum by TSR can produce naphthenic acids

(Machel, 2001), which are effective ligands for the complexation and transport of Zn in petroleum (Sanz-Robinson and Williams-Jones, 2019).

We propose that residual reduced sulfur-enriched hydrocarbons in the Sichuan basin supplied the Ni (and Pd, Pt, Os, Au, Zn and Mo), which formed the hyper-enriched black shale Ni deposits in southern China. The presence of highly enriched bituminous veins below the Nick prospect suggests that the HEBS in Yukon Canada had a similar history. According to the above hypothesis, the formation of HEBS is genetically related to a large petroleum system that undergoes pulses of thermal cracking and TSR (Cai et. al., 2004; Hu et. al., 2010) yielding natural gas, sour gas and residual petroleum enriched in thiols. With consumption of the petroleum by TSR, the volume of residual oil shrinks but becomes increasingly enriched in thiols and it is this oil that supplies the Ni (and other metals), which distinguishes hyper-enriched black shale deposits from other sediment-hosted metalliferous deposits.

Further evidence for the involvement of liquid hydrocarbons in the formation of HEBS, is provided by the (circa 2.0 – 1.9 Ga) Talvivaara deposit in Finland, which hosts significant Ni reserves, and contains uraninite crystals rimmed by bitumen. The latter indicates that hydrocarbons, possibly from source rocks deeper in the stratigraphy deposited during the Shunga event (c. 2.0 Ga), migrated through the deposit (Lecomte et al, 2014). This event was marked by the global deposition of organic carbon-rich rocks and the development of vast petroleum resources such as those in Zaonezhskaya Formation of the Onega Basin in Russian Fennoscandia (Melezhik et al, 2009, Asael et al., 2013; Strauss et al., 2013; Lecomte et al, 2014). Thus, not only is the mineralization in the Talvivaara deposit associated with bitumen, but there was also a

large reservoir of liquid hydrocarbons, which could have transported the metals to the site of ore formation.

As mentioned above, one of the currently favored hypotheses for the HEBS of southern China and the Yukon, Canada is that they are synsedimentary and formed as a result of the precipitation of the ore metals from seawater (seawater contains 2 ppb Ni on average; Kato et. al., 1990) at the seawater-sediment interface through bacterially-mediated processes. It has been suggested that textures of the iron sulfides (i.e. framboidal pyrite) at the HEBS of Yukon, Canada reflect deposition during early-diagenesis (Gadd et. al., 2018, and 2019). However, pyritic framboids could have also formed abiotically (Scott et. al., 2009) and the millerite (NiS) mineralization at the Peel River HEBS in Yukon, show it mantling and replacing pyrite (Henderson et al., 2019), indicating that the nickel mineralization is epigenetic. Finally, the required concentration factor (~ 10 million; from 2 ppb to several wt%) seems unreasonably high. The other hypothesis for the formation of HEBS, namely that they are epigenetic but deposited from saline hydrothermal-vent brines (Lott et. al., 1999, Steiner et. al., 2001), is also problematic. This is because Ni is highly insoluble in hydrothermal fluids, even those with high chloride activity, making it unlikely that saline brines could have constituted an ore fluid for the mineralization in these rocks. For example, at 250 °C and fO_2-pH conditions buffered by the assemblage magnetite-pyrite-pyrrhotite, the solubility of millerite, the main Ni mineral in HEBS deposits, is 0.2 ppm; this solubility decreases with decreasing temperature (Liu et. al., 2012). In view of the serious weaknesses of the synsedimentary seawater and epigenetic brine models, the role of petroleum as an ore fluid for Ni and other metals in sediment-hosted deposits merits serious consideration.

5 Conclusions

The potential of liquid hydrocarbons to act as ore fluids was evaluated by reacting Ni wires in crude oil at elevated temperature (150-250°C). Below 150°C, Ni concentrations in the three crude oils considered in this study remained relatively low. Above, 200 °C, one of the oils, (Oil C) dissolved considerably more Ni than the other two oils (reaching a concentration of 217 ppm at 250°C). X-ray photoelectron spectroscopic analyses of the residual oil coating the Ni wires after reaction indicates that Ni has a strong chemical affinity for thiols. This is supported by the observation that Oil C, the most Ni-philic of the oils has the highest thiol content (52 ppm). Oil A, which has the second highest thiol concentration (44 ppm), dissolved the second largest amount of Ni (up to 26 ppm Ni at 200°C). The much lower capacity of Oil A to dissolve Ni compared to Oil C and its only slightly lower thiol content, however, indicate that a second species played an important role in Ni solubility. As Oil C has the highest nitrogen content (0.44 wt.%) of the three oils and Oil A contains no nitrogen, this second species is likely to be a Ni-porphyrin, which previous studies have linked to the high concentration of Ni in some crude oils. Oil C also has a high carboxylic acid content (indicated by its high TAN value), whereas that of Oil A is very low (very low TAN value). This much higher acidity of Oil C compared to Oil A may have promoted the stronger binding of Ni to thiol ligands and the formation of Ni-thiolate complexes, thereby further explaining the much higher capacity of Oil C to dissolve Ni; Ni-thiolation may also be promoted by the presence of Fe as shown by the synchronous incorporation of Fe in the Ni wires and the binding of thiols to them. The evidence that liquid hydrocarbons can dissolve high concentrations of Ni, that Ni is extremely insoluble in hydrothermal fluids and that Ni forms ore deposits (several wt.% Ni) in black shales, which have

been infiltrated by petroleum, makes a compelling case that liquid hydrocarbons could be important ore fluids for nickel.

Acknowledgments

The research described in this paper was funded by a grant from Statoil Canada and a collaborative research and development grant from NSERC. The crude oil samples used in the experiments were supplied by Statoil Canada. We thank Scott Bohle and Danae Guerra for their assistance with our X-Ray Photoelectron Spectroscopy analyses and Ichiko Sugiyama for her help in setting-up the solubility experiments. Constructive comments by Mike Gadd and an anonymous Chemical Geology reviewer helped improve the manuscript substantially.

References

Ali, M.F., Perzanowski, H., Bukhari, A. and Al-Haji, A.A., 1993. Nickel and vanadyl porphyrins in Saudi Arabian crude oils. *Energy & Fuels*, *7*(2), pp.179-184.

Asael, D., Tissot, F.L., Reinhard, C.T., Rouxel, O., Dauphas, N., Lyons, T.W., Ponzevera, E., Liorzou, C. and Chéron, S., 2013. Coupled molybdenum, iron and uranium stable isotopes as oceanic paleoredox proxies during the Paleoproterozoic Shunga Event. *Chemical Geology*, *362*, pp.193-210.

Barwise, A.J.G., 1990. Role of nickel and vanadium in petroleum classification. *Energy & Fuels*, *4*(6), pp.647-652.

Bechtel, A. and Püttmann, W., 1991. The origin of the Kupferschiefer-type mineralization in the Richelsdorf Hills, Germany, as deduced from stable isotope and organic geochemical studies. *Chemical Geology*, *91*(1), p.1-18.

Belkin, H.E. and Luo, K., 2008. Late-stage sulfides and sulfarsenides in Lower Cambrian black shale (stone coal) from the Huangjiawan mine, Guizhou Province, People's Republic of China. *Mineralogy and Petrology*, *92*(3-4), pp.321-340.

Cai, C., Worden, R.H., Bottrell, S.H., Wang, L. and Yang, C., 2003. Thermochemical sulphate reduction and the generation of hydrogen sulphide and thiols (mercaptans) in Triassic carbonate reservoirs from the Sichuan Basin, China. *Chemical Geology*, *202*(1-2), pp.39-57

Cai, C., Xie, Z., Worden, R.H., Hu, G., Wang, L. and He, H., 2004. Methane-dominated thermochemical sulphate reduction in the Triassic Feixianguan Formation East Sichuan Basin, China: towards prediction of fatal H2S concentrations. *Marine and Petroleum Geology*, *21*(10), pp.1265-1279.

Caineng, Z., Jinhu, D.U., Chunchun, X.U., Zecheng, W.A.N.G., Zhang, B., Guoqi, W., Tongshan, W., Genshun, Y., Shenghui, D., Jingjiang, L. and Hui, Z., 2014. Formation,

distribution, resource potential, and discovery of Sinian–Cambrian giant gas field, Sichuan Basin, SW China. *Petroleum Exploration and Development*, *41*(3), pp.306-325.

Castner, D.G., Hinds, K. and Grainger, D.W., 1996. X-ray photoelectron spectroscopy sulfur 2p study of organic thiol and disulfide binding interactions with gold surfaces. *Langmuir*, *12*(21), p.5083-5086.

Caumette, G., Lienemann, C.P., Merdrignac, I., Bouyssiere, B. and Lobinski, R., 2009. Element speciation analysis of petroleum and related materials. *Journal of Analytical Atomic Spectrometry*, *24*(3), pp.263-276.

Clegg, W. and Henderson, R.A., 2002. Kinetic evidence for intramolecular proton transfer between nickel and coordinated thiolate. *Inorganic chemistry*, *41*(5), pp.1128-1135.

Diekert, G., Konheiser, U., Piechulla, K. and Thauer, R.K., 1981. Nickel requirement and factor F430 content of methanogenic bacteria. *Journal of Bacteriology*, *148*(2), pp.459-464.

EIA, 2011. World Shale Gas Resources: an Initial Assessment of 14 Regions Outside the United States. U.S. Department of Energy, Washington. DC.

Fish, R.H., Komlenic, J.J. and Wines, B.K., 1984. Characterization and comparison of vanadyl and nickel compounds in heavy crude petroleums and asphaltenes by reverse-phase and size-

exclusion liquid chromatography/graphite furnace atomic absorption spectrometry. *Analytical Chemistry*, *56*(13), pp.2452-2460.

Gadd, M.G. and Peter, J.M., 2017. Field observations, mineralogy and geochemistry of Middle Devonian Ni-Zn-Mo-PGE hyper-enriched black shale deposits, Yukon. *Targeted Targeted Geoscience Initiative*.

Gadd, M. G., and Peter, J. M., 2018, Field observations, mineralogy and geochemistry of Middle Devonian Ni-Zn-Mo-PGE hyper-enriched black shale deposits, *Yukon, in Rogers, N., ed., Targeted Geoscience Initiative: 2017 report of activities, volume 1; Geological Survey of Canada*, Open File 8358, p. 193-206.

Gadd, M. G., Peter, J. M., Jackson, S. E., Yang, Z., and Petts, D., 2019, Platinum, Pd, Mo, Au and Re deportment in hyper-enriched black shale Ni-Zn-Mo-PGE mineralization, Peel River, Yukon, Canada: *Ore Geology Reviews*, v. 107, p. 600-614.

Giordano, T.H., 1994, Metal Transport in Ore Fluids by Organic Ligand Complexation, *in* Pittman, E.D. and Lewan, M.D. eds., Organic Acids in Geological Processes, Springer-Verlag, p. 320 – 354.

Groenzin, H. and Mullins, O.C., 1999. Asphaltene molecular size and structure. *The Journal of Physical Chemistry A*, *103*(50), pp.11237-11245.

Grotzinger, J.P., Fike, D.A. and Fischer, W.W., 2011. Enigmatic origin of the largest-known carbon isotope excursion in Earth's history. *Nature Geoscience*, *4*(5), p.285.

Hao, F., Guo, T., Zhu, Y., Cai, X., Zou, H. and Li, P., 2008. Evidence for multiple stages of oil cracking and thermochemical sulfate reduction in the Puguang gas field, Sichuan Basin, China. *AAPG bulletin*, *92*(5), pp.611-637.

Hao, F., Zhang, X., Wang, C., Li, P., Guo, T., Zou, H., Zhu, Y., Liu, J. and Cai, Z., 2015. The fate of CO2 derived from thermochemical sulfate reduction (TSR) and effect of TSR on carbonate porosity and permeability, Sichuan Basin, China. *Earth-Science Reviews*, *141*, pp.154-177.

Head, I.M., Jones, D.M. and Larter, S.R., 2003. Biological activity in the deep subsurface and the origin of heavy oil. *Nature*, *426*(6964), p.344.

Henderson, K.M., Williams-Jones, A.E., and Clark, J.R., 2019. Metal transport by liquid hydrocarbons: Evidence from metalliferous shale and pyrobitumen, Yukon; in *Targeted Geoscience Initiative: 2018 report of activities, (ed.) N. Rogers; Geological Survey of Canada*, Open File 8549, p. 179-187.

Ho, T.Y., Rogers, M.A., Drushel, H.V. and Koons, C.B., 1974. Evolution of sulfur compounds in crude oils. *AAPG Bulletin*, *58*(11), p.2338-2348.

Hodgson, G.W., 1973. Geochemistry of porphyrins—reactions during diagenesis. *Annals of the New York Academy of Sciences*, *206*(1), pp.670-684.

Hu, A., Li, M., Wong, J., Reyes, J., Achal, S., Milovic, M., Robinson, R., Shou, J., Yang, C., Dai, J. and Ma, Y., 2010. Chemical and petrographic evidence for thermal cracking and thermochemical sulfate reduction of paleo-oil accumulations in the NE Sichuan Basin, China. *Organic geochemistry*, *41*(9), pp.924-929.

Hughey, C.A., Rodgers, R.P., Marshall, A.G., Walters, C.C., Qian, K. and Mankiewicz, P., 2004. Acidic and neutral polar NSO compounds in Smackover oils of different thermal maturity revealed by electrospray high field Fourier transform ion cyclotron resonance mass spectrometry. *Organic geochemistry*, *35*(7), pp.863-880.

Hulbert, L.J., Carne, R.C., Gregoire, D.C. and Paktunc, D., 1992. Sedimentary nickel, zinc, and platinum-group-element mineralization in Devonian black shales at the Nick Property, Yukon, Canada; a new deposit type. *Exploration and Mining Geology*, *1*(1), pp.39-62.

Hulen, J.B. and Collister, J.W., 1999. The oil-bearing, carlin-type gold deposits of Yankee Basin, Alligator Ridge District, Nevada. *Economic Geology*, *94*(7), pp.1029-1049.

Jiang, G., Kaufman, A.J., Christie-Blick, N., Zhang, S. and Wu, H., 2007. Carbon isotope variability across the Ediacaran Yangtze platform in South China: Implications for a large

surface-to-deep ocean δ13C gradient. *Earth and Planetary Science Letters*, *261*(1-2), pp.303-320.

Jowett, E.C., Roth, T., Rydzewski, A. and Oszczepalski, S., 1991. "Background" δ 34 S values of Kupferschiefer sulphides in Poland: pyrite-marcasite nodules. *Mineralium Deposita*, *26*(2), p.89-98.

Jowitt, S.M. and Keays, R.R., 2011. Shale-hosted Ni–(Cu–PGE) mineralisation: a global overview. *Applied Earth Science*, *120*(4), pp.187-197.

Kapo, G.: Vanadium: key to Venezuelan fossil hydrocarbons. In: Bitumens, asphalts and tar sands, G. V. Chilingarian, T. F. Yen, Eds., pp. 155-190. Amsterdam: Elsevier 1978.

Kato, T., Nakamura, S. and Morita, M., 1990. Determination of nickel, copper, zinc, silver, cadmium and lead in seawater by isotope dilution inductively coupled plasma mass spectrometry. *Analytical Sciences*, *6*(4), pp.623-626.

Kelemen, S.R., George, G.N. and Gorbaty, M.L., 1990. Direct determination and quantification of organic sulfur forms by X-ray photoelectron spectroscopy (XPS) and sulfur k-edge absorption spectroscopy. *Fuel Processing Technology*, *24*, pp.425-429.

Kelly, W.C. and Nishioka, G.K., 1985. Precambrian oil inclusions in late veins and the role of hydrocarbons in copper mineralization at White Pine, Michigan. *Geology*, *13*(5), pp.334-337.

Kříbek, B., Sýkorová, I., Pašava, J. and Machovič, V., 2007. Organic geochemistry and petrology of barren and Mo–Ni–PGE mineralized marine black shales of the Lower Cambrian Niutitang Formation (South China). *International Journal of Coal Geology*, *72*(3-4), pp.240-256.

Korsch, R.J., Huazhao, M., Zhaocai, S. and Gorter, J.D., 1991. The Sichuan basin, southwest China: a late proterozoic (Sinian) petroleum province. *Precambrian Research*, *54*(1), pp.45-63.

Lambert, I.B., Walter, M.R., Wenlong, Z., Songnian, L. and Guogan, M.A., 1987. Palaeoenvironment and carbon isotope stratigraphy of Upper Proterozoic carbonates of the Yangtze Platform. *Nature*, *325*(6100), p.140.

Lan, Z., Li, X.H., Chu, X., Tang, G., Yang, S., Yang, H., Liu, H., Jiang, T. and Wang, T., 2017. SIMS U-Pb zircon ages and Ni-Mo-PGE geochemistry of the lower Cambrian Niutitang Formation in South China: Constraints on Ni-Mo-PGE mineralization and stratigraphic correlations. *Journal of Asian Earth Sciences*, *137*, pp.141-162.

Langevin, D., Poteau, S., Hénaut, I. and Argillier, J.F., 2004. Crude oil emulsion properties and their application to heavy oil transportation. *Oil & gas science and technology*, *59*(5), pp.511-521.

Lecomte, A., Cathelineau, M., Deloule, E., Brouand, M., Peiffert, C., Loukola-Ruskeeniemi, K., Pohjolainen, E. and Lahtinen, H., 2014. Uraniferous bitumen nodules in the Talvivaara Ni–Zn–

Cu–Co deposit (Finland): influence of metamorphism on uranium mineralization in black shales. *Mineralium Deposita*, *49*(4), pp.513-533.

Lehmann, B., Frei, R., Xu, L. and Mao, J., 2016. Early Cambrian black shale-hosted Mo-Ni and V mineralization on the rifted margin of the Yangtze Platform, China: reconnaissance chromium isotope data and a refined metallogenic model. *Economic Geology*, *111*(1), pp.89-103.

Lewan, M., 1984, Factors controlling the proportionality of vanadium to nickel in crude oils: Geochimica et Cosmochimica Acta, v. 48, p. 2231 – 2238.

Liu, W., Migdisov, A. and Williams-Jones, A., 2012. The stability of aqueous nickel (II) chloride complexes in hydrothermal solutions: Results of UV–Visible spectroscopic experiments. *Geochimica et Cosmochimica Acta*, *94*, pp.276-290.

Lott, D.A., Coveney, R.M., Murowchick, J.B. and Grauch, R.I., 1999. Sedimentary exhalative nickel-molybdenum ores in South China. *Economic Geology*, *94*(7), pp.1051-1066.

Loukola-Ruskeeniemi, K. and Heino, T., 1996. Geochemistry and genesis of the black shale-hosted Ni-Cu-Zn deposit at Talvivaara, Finland. *Economic Geology*, *91*(1), pp.80-110.

Lingang, X., Lehmann, B., Jingwen, M., Wenjun, Q. and Andao, D., 2011. Re-Os age of polymetallic Ni-Mo-PGE-Au mineralization in Early Cambrian black shales of South China—a reassessment. *Economic Geology*, *106*(3), pp.511-522.

Machel, H.G., 2001. Bacterial and thermochemical sulfate reduction in diagenetic settings—old and new insights. *Sedimentary Geology*, *140*(1-2), pp.143-175.

Marcano, F., Flores, R., Chirinos, J. and Ranaudo, M.A., 2011. Distribution of Ni and V in A1 and A2 asphaltene fractions in stable and unstable Venezuelan crude oils. *Energy & Fuels*, *25*(5), pp.2137-2141.

McFadden, K.A., Huang, J., Chu, X., Jiang, G., Kaufman, A.J., Zhou, C., Yuan, X. and Xiao, S., 2008. Pulsed oxidation and biological evolution in the Ediacaran Doushantuo Formation. *Proceedings of the National Academy of Sciences*, *105*(9), pp.3197-3202.

Melezhik, V.A., Fallick, A.E., Filippov, M.M., Lepland, A., Rychanchik, D.V., Deines, Y.E., Medvedev, P.V., Romashkin, A.E. and Strauss, H., 2009. Petroleum surface oil seeps from a Palaeoproterozoic petrified giant oilfield. *Terra Nova*, *21*(2), pp.119-126.

Meyer, R. F. (1989). Heavy oil and natural bitumen. *The Petroleum System: Status of Research and methods, 1990"*, U.S.G.P.O. pp 64.

Mitra-Kirtley, S., Mullins, O.C., Van Elp, J., George, S.J., Chen, J. and Cramer, S.P., 1993. Determination of the nitrogen chemical structures in petroleum asphaltenes using XANES spectroscopy. *Journal of the American Chemical society*, *115*(1), pp.252-258.

Nguyen, V.P., Burklé-Vitzthum, V., Marquaire, P.M. and Michels, R., 2013. Thermal reactions between alkanes and H2S or thiols at high pressure. *Journal of analytical and applied pyrolysis*, *103*, pp.307-319.

Ohki, Y. and Tatsumi, K., 2011. Thiolate-Bridged Iron–Nickel Models for the Active Site of [NiFe] Hydrogenase. *European Journal of Inorganic Chemistry*, *2011*(7), pp.973-985.

Orberger, B., Vymazalova, A., Wagner, C., Fialin, M., Gallien, J.P., Wirth, R., Pasava, J. and Montagnac, G., 2007. Biogenic origin of intergrown Mo-sulphide-and carbonaceous matter in Lower Cambrian black shales (Zunyi Formation, southern China). *Chemical geology*, *238*(3-4), pp.213-231.

Orr, W.L., 1986. Kerogen/asphaltene/sulfur relationships in sulfur-rich Monterey oils. *Organic geochemistry*, *10*(1-3), pp.499

Oswald, A.A., 1961. Organic Sulfur Compounds. III. Co-Oxidation of Mercaptans with Styrenes and Indene. *The Journal of Organic Chemistry*, *26*(3), pp.842-846.

Oszczepalski, S., Nowak, G., Bechtel, A. and Zák, K., 2012. Evidence of oxidation of the Kupferschiefer in the Lubin-Sieroszowice deposit, Poland: implications for Cu-Ag and Au-Pt-Pd mineralisation. *Geological Quarterly*, *46*(1), p.1-24.

Pages, A., Barnes, S., Schmid, S., Coveney Jr, R.M., Schwark, L., Liu, W., Grice, K., Fan, H. and Wen, H., 2018. Geochemical investigation of the lower Cambrian mineralised black shales of South China and the late Devonian Nick deposit, Canada. *Ore Geology Reviews*, *94*, pp.396-413.

Parnell, J., 1988. Metal enrichments in solid bitumens: a review. *Mineralium Deposita*, *23*(3), pp.191-199.

Parnell, J. and Eakin, P., 1987. The replacement of sandstones by uraniferous hydrocarbons: significance for petroleum migration. *Mineralogical Magazine*, *51*(362), pp.505-515.

Peabody, C.E. and Einaudi, M.T., 1992. Origin of petroleum and mercury in the Culver-Baer cinnabar deposit, Mayacmas district, California. *Economic Geology*, *87*(4), pp.1078-1103.

Pearson, G., 1963. Hard and Soft Acids and Bases: Journal of the American Chemical Society, 85, p. 3533–3539.

Peter, J.M., and Scott, S.D., 1988, Mineralogy, composition, and fluid-inclusion microthermometry of seafloor hydrothermal deposits in the Southern Trough of Guaymas Basin, Gulf of California: Canadian Mineralogist, v. 26, p. 567–587.

Peters, K.E., Walters, C.C., and Moldowan, J.M., 2004, The Biomarker Guide: Volume 1, Biomarker and Isotopes in the Environment and Human History: Cambridge University Press.

Price, L.C., and Wenger, L.M., 1992, The influence of pressure on petroleum generation and maturation as suggested by aqueous pyrolysis: Organic Geochemistry, v. 19, p. 141–159.

Potočnik, J., Nenadović, M., Jokić, B.M., Popović, M. and Rakočević, Z.L., 2016. Properties of Zig-Zag Nickel Nanostructures Obtained by GLAD Technique. *Science of Sintering*, *48*(1), pp.51-56

Ragsdale, S.W., 2009. Nickel-based enzyme systems. *Journal of Biological Chemistry*, *284*(28), pp.18571-18575.

Saintilan, N.J., Spangenberg, J.E., Chiaradia, M., Chelle-Michou, C., Stephens, M.B. and Fontboté, L., 2019. Petroleum as source and carrier of metals in epigenetic sediment-hosted mineralization. *Scientific reports*, *9*(1), p.8283.

Sanz-Robinson, J. and Williams-Jones, A.E., 2019. Zinc solubility, speciation and deposition: A role for liquid hydrocarbons as ore fluids for Mississippi Valley Type Zn-Pb deposits. *Chemical Geology*, *520*, pp.60-68.

Sanz-Robinson, J., Sugiyama, I., and Williams-Jones A.E., (Accepted for publication). The Solubility of Palladium (Pd) in Crude Oil at 150, 200 and 250 °C and its Application to Ore Genesis. *Chemical Geology*

Scott, R.J., Meffre, S., Woodhead, J., Gilbert, S.E., Berry, R.F. and Emsbo, P., 2009. Development of framboidal pyrite during diagenesis, low-grade regional metamorphism, and hydrothermal alteration. *Economic Geology*, *104*(8), pp.1143-1168.

Seifert, W.K., 1975. Carboxylic acids in petroleum and sediments. In: Fortschritte der Chemie Organischer Naturstoffe/Progress in the Chemistry of Organic Natural Products. Springer, Vienna, pp. 1–49.

Speight, J.G., 2001, Handbook of Petroleum Analysis (J. G. Speight, Ed.): John Wiley & Sons, Inc.

Steiner, M., Wallis, E., Erdtmann, B.D., Zhao, Y., and Yang, R., 2001. Submarine-hydrothermal exhalative ore layers in black shales from South China and associated fossils - Insights into a Lower Cambrian facies and bio-evolution; *Palaeogeography, Palaeoclimatology, Palaeoecology*, v. 169, p. 165–191.

Strauss, H., Melezhik, V.A., Lepland, A., Fallick, A.E., Hanski, E.J., Filippov, M.M., Deines, Y.E., Illing, C.J., Črne, A.E. and Brasier, A.T., 2013. 7.6 Enhanced Accumulation of Organic Matter: The Shunga Event. In *Reading the archive of Earth's oxygenation* (pp. 1195-1273). Springer, Berlin, Heidelberg.

Sugihara, J.M. and Bean, R.M., 1962. Direct determination of metalloporphyrins in Boscan crude oil. *Journal of Chemical and Engineering Data*, *7*(2), pp.269-271.

Sugiyama, I. and Williams-Jones, A.E., 2018. An approach to determining nickel, vanadium and other metal concentrations in crude oil. *Analytica chimica acta*, *1002*, pp.18-25.

Summons, R.E. and Powell, T.G., 1992. Hydrocarbon composition of the Late Proterozoic oils of the Siberian Platform: Implications for the depositional environment of source rocks. In *Early Organic Evolution* (pp. 296-307). Springer, Berlin, Heidelberg.

Sun, Y.Z., 1998. Influences of secondary oxidation and sulfide formation on several maturity parameters in Kupferschiefer. *Organic Geochemistry*, *29*(5-7), pp.1419-1429.

Wagner, C.D., 1972. Auger lines in x-ray photoelectron spectrometry. *Analytical Chemistry*, *44*(6), pp.967-973.

Wang, G., Wang, T.G., Han, K., Wang, L. and Shi, S., 2015. Recognition of a novel Precambrian petroleum system based on isotopic and biomarker evidence in Yangtze platform, South China. *Marine and Petroleum Geology*, *68*, pp.414-426.

Wei, Z., Mankiewicz, P., Walters, C., Qian, K., Phan, N.T., Madincea, M.E. and Nguyen, P.T., 2011. Natural occurrence of higher thiadiamondoids and diamondoidthiols in a deep petroleum reservoir in the Mobile Bay gas field. *Organic geochemistry*, *42*(2), pp.121-133.

Wenger, L.M., Davis, C.L. and Isaksen, G.H., 2002. Multiple controls on petroleum biodegradation and impact on oil quality. *SPE Reservoir Evaluation & Engineering*, *5*(05), pp.375-383.

Williams-Jones, A.E., Bowell, R.J. and Migdisov, A.A., 2009. Gold in solution. *Elements*, *5*(5), pp.281-287.

Williams-Jones, A.E. and Migdisov, A.A., 2014. Experimental constraints on the transport and deposition of metals in ore-forming hydrothermal systems. *Society of Economic Geologists*, *18*, pp.77-96.

Worden, R.H., Smalley, P.C. and Cross, M.M., 2000. The influence of rock fabric and mineralogy on thermochemical sulfate reduction: Khuff Formation, Abu Dhabi. *Journal of Sedimentary Research*, *70*(5), pp.1210-1221.

Young, S.A., Loukola-Ruskeeniemi, K. and Pratt, L.M., 2013. Reactions of hydrothermal solutions with organic matter in Paleoproterozoic black shales at Talvivaara, Finland: Evidence from multiple sulfur isotopes. *Earth and Planetary Science Letters*, *367*, pp.1-14.

Yu, C., Zhang, L., Guo, X., Xu, Z., Sun, X., Xu, C. and Zhao, S., 2015. Association model for nickel and vanadium with asphaltene during solvent deasphalting. *Energy & Fuels*, *29*(3), pp.1534-1542.

Zhu, G., Wang, T., Xie, Z., Xie, B. and Liu, K., 2015. Giant gas discovery in the Precambrian deeply buried reservoirs in the Sichuan Basin, China: Implications for gas exploration in old cratonic basins. *Precambrian Research*, *262*, pp.45-66.

Zou, C., Wei, G., Xu, C., Du, J., Xie, Z., Wang, Z., Hou, L., Yang, C., Li, J. and Yang, W., 2014. Geochemistry of the Sinian–Cambrian gas system in the Sichuan Basin, China. *Organic geochemistry*, *74*, pp.13-21.

Appendix

A. Calculation of the thiol content of the Rodney Crude oil

$API = \frac{141.5}{SG} - 131.5$, where API is a measure of the weight of petroleum liquids and SG is the specific gravity of the oil.

Therefore, $SG = \frac{141.5}{API+131.5}$

The API value for the Rodney Crude is 32. (Ho et al., 1974)

$SG_{Rodney\ Crude} = \frac{141.5}{32+131.5} = 0.865$

$SG = \frac{\rho_{Oil}}{\rho_{H2O}}$ where ρ denominates density.

Assuming $\rho_{H2O} = 1.0$ g/mL

$\rho_{Rodney\ Crude} = SG_{Rodney\ Crude} = 0.865$ g/mL

Mercaptan Number= $\frac{mg\ of\ thiol\ S}{100mL}$ (Oswald, 1961)

The Mercaptan number for the Rodney Crude is 275 (Ho et al., 1974)

Mercaptan Number= $\frac{275\ mg\ of\ thiol\ S}{100mL} = \frac{275\ mg\ thiol\ S\ x\ \frac{1000\mu g}{mg}}{100mL\ x\ \rho_{Rodney\ Crude}} = \frac{275000\ \mu g}{100mL\ x\ \frac{0.865g}{mL}} = 3179\ ppm$

Thus, the Rodney Crude contains 3179 ppm of thiol S.

B. Supplementary Figures

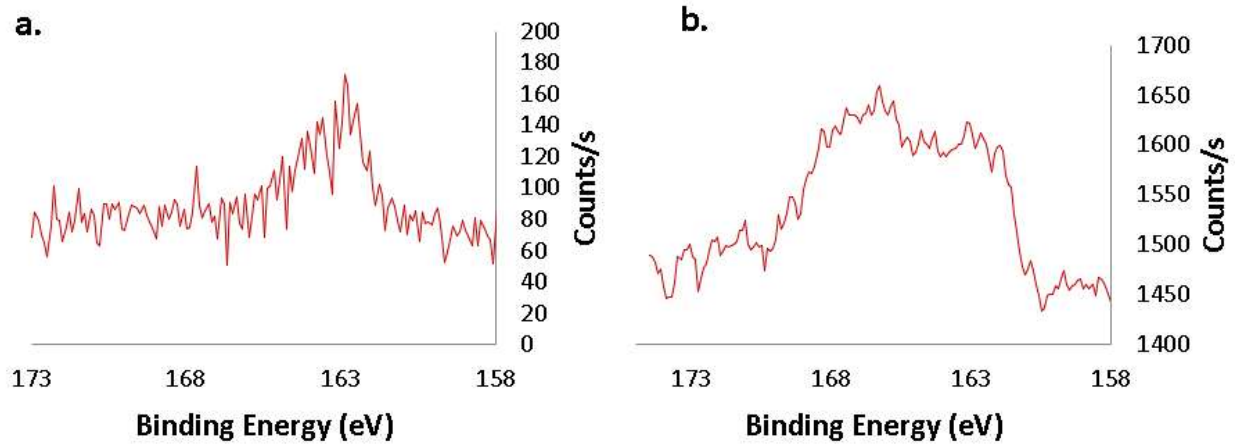

Figure A1. X-ray photoelectron spectra of the residual oil left on the Ni wire after reaction with Oil A at a) 200° and b) ambient temperature.

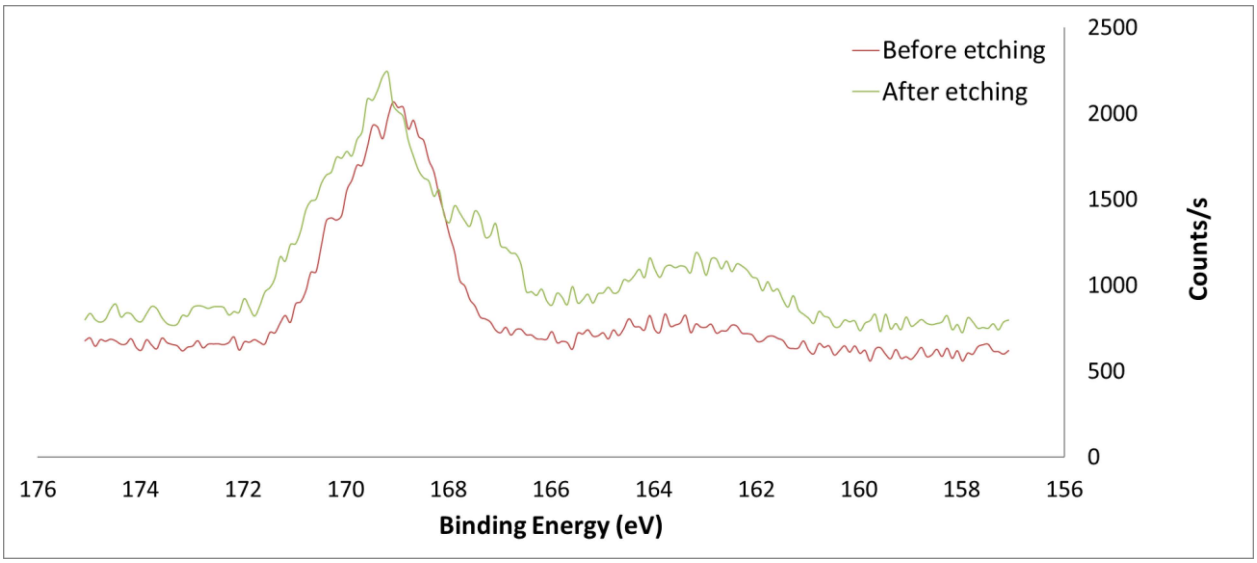

Figure A2. Sulfur (S2p) XPS of the residual oil left on the Ni wire after reaction with Oil A at 150°C before and after etching.

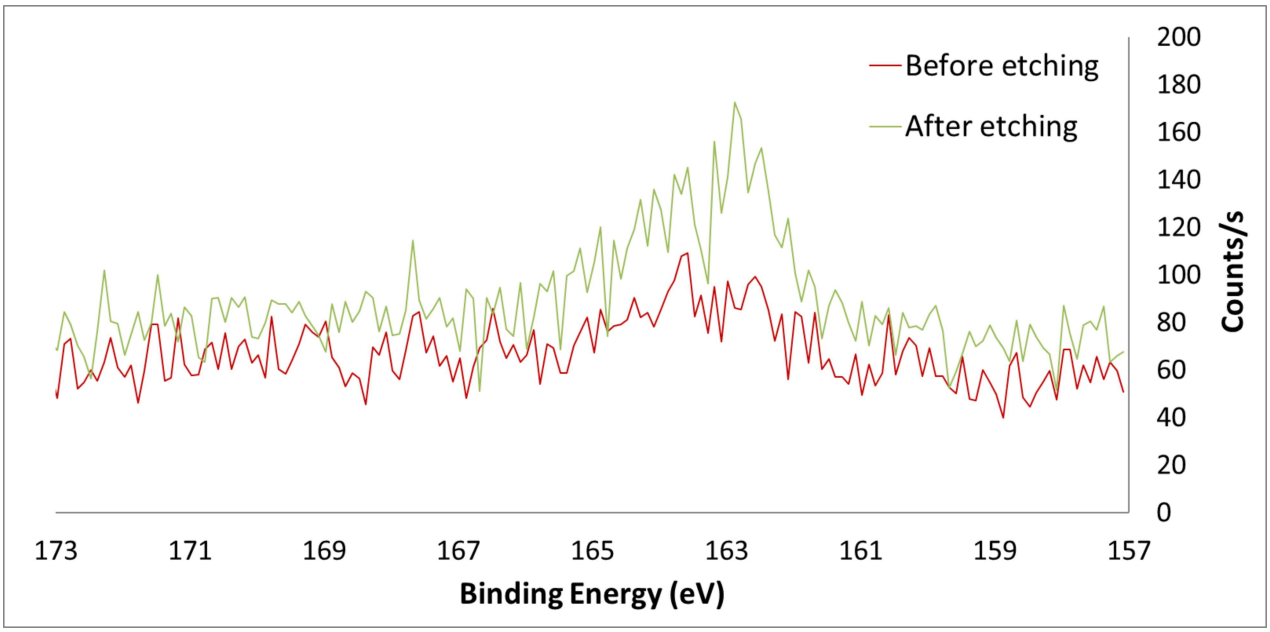

Figure A3. Sulfur (S2p) XPS of the residual oil left on the Ni wire after reaction with Oil A at 200°C before and after etching.

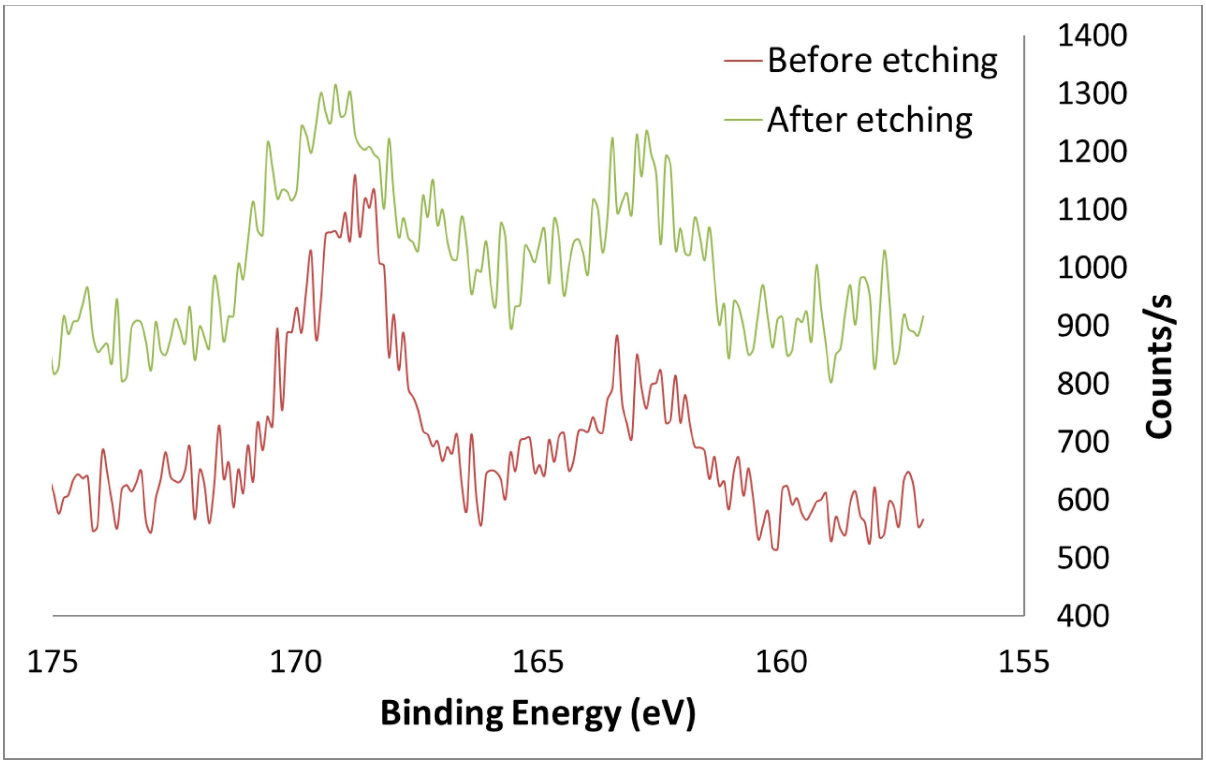

Figure A4. Sulfur (S2p) XPS of the residual oil left on the Ni wire after reaction with Oil B at 150°C before and after etching.

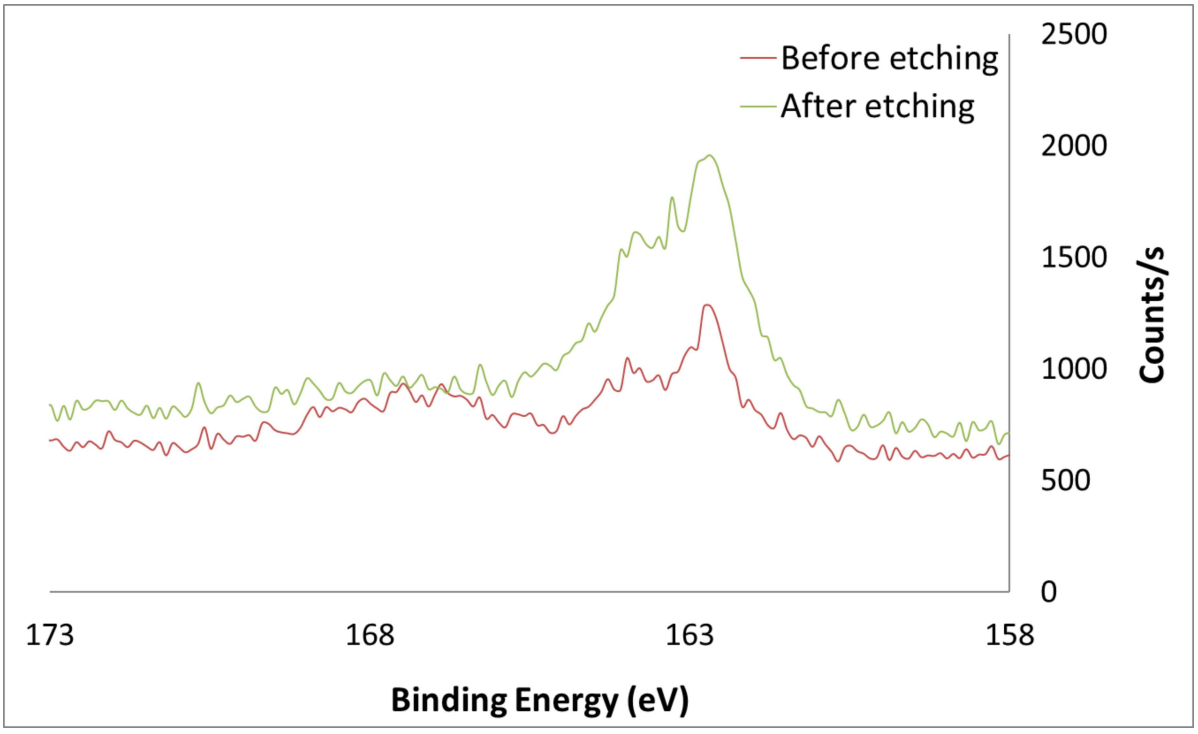

Figure A5. Sulfur (S2p) XPS of the residual oil left on the Ni wire after reaction with Oil B at 200°C before and after etching.

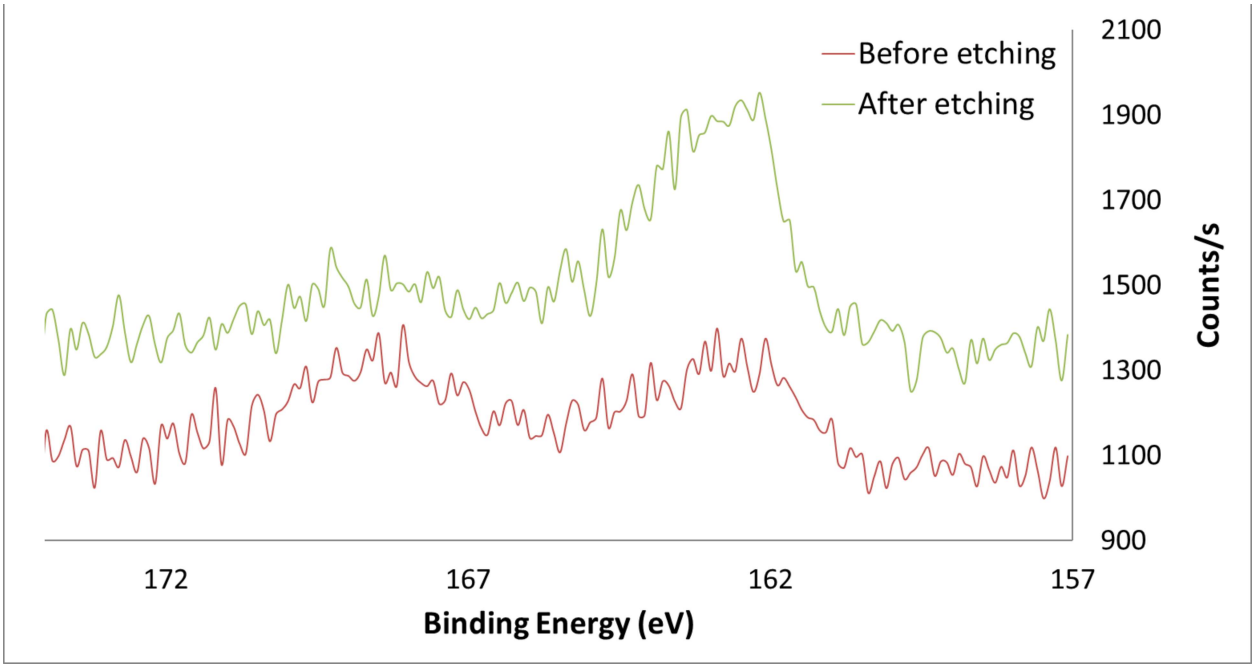

Figure A6. Sulfur (S2p) XPS of the residual oil left on the Ni wire after reaction with Oil C at 150°C before and after etching.

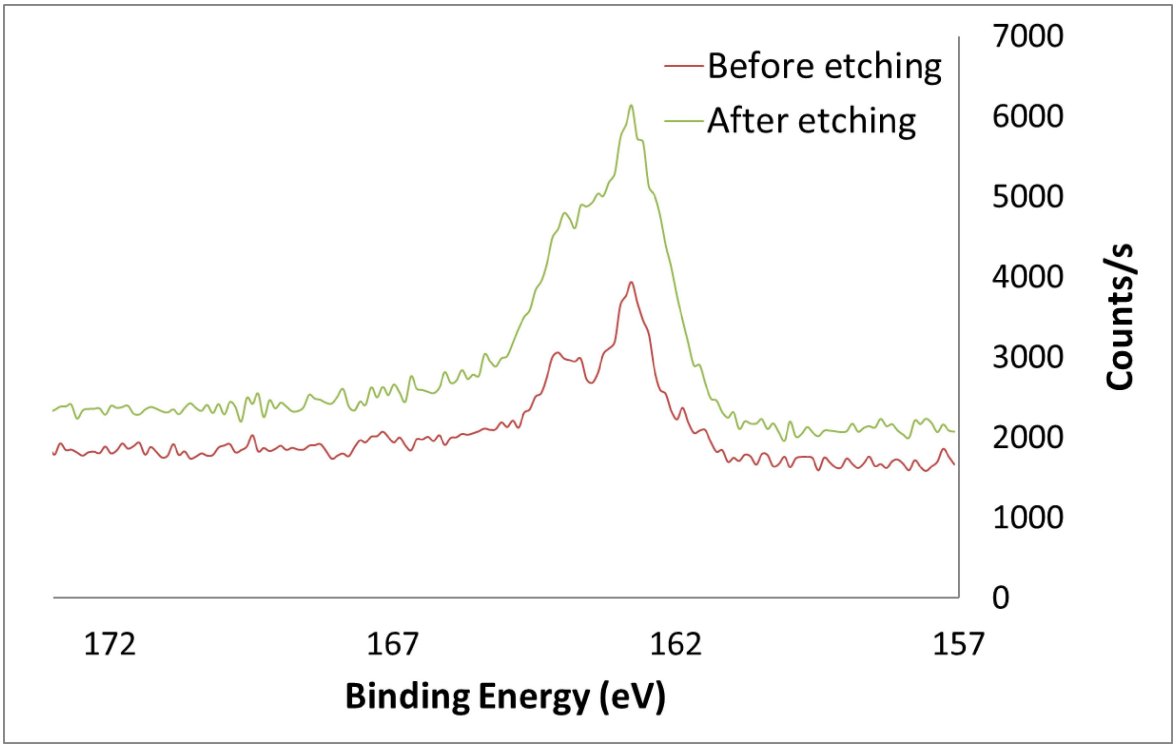

Figure A7. Sulfur (S2p) XPS of the residual oil left on the Ni wire after reaction with Oil C at 200°C before and after etching.

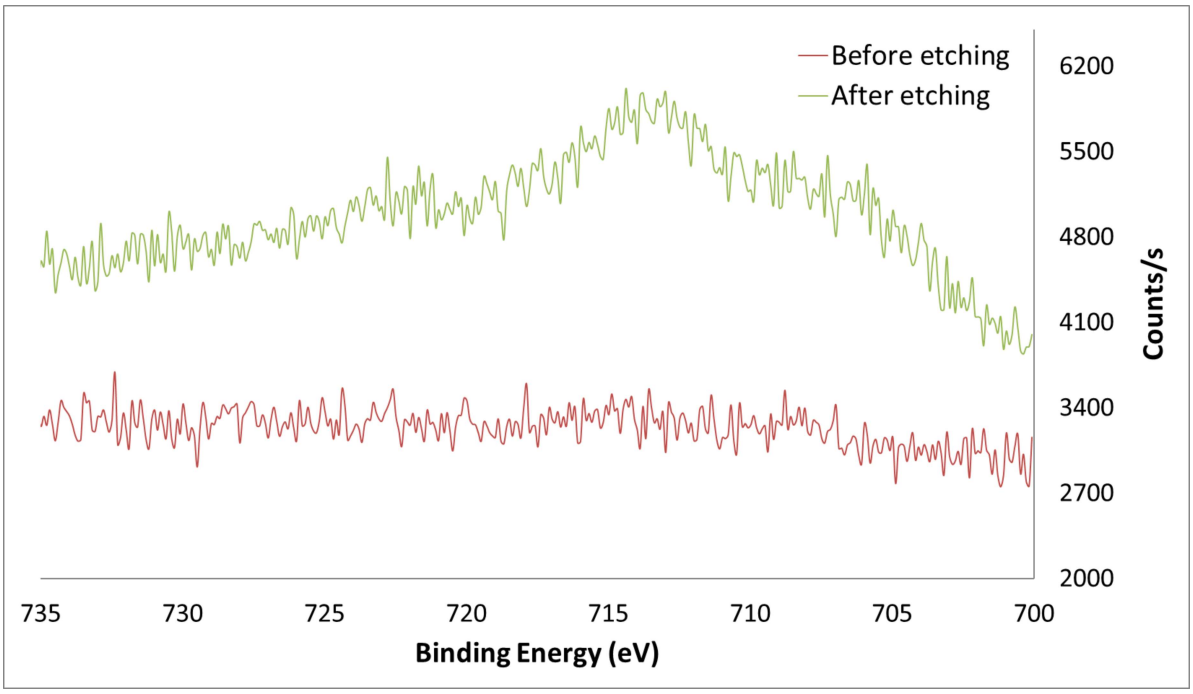

Figure A8. Iron (Fe2p) XPS of the residual oil left on the Ni wire after reaction with Oil A at 150°C before and after etching.

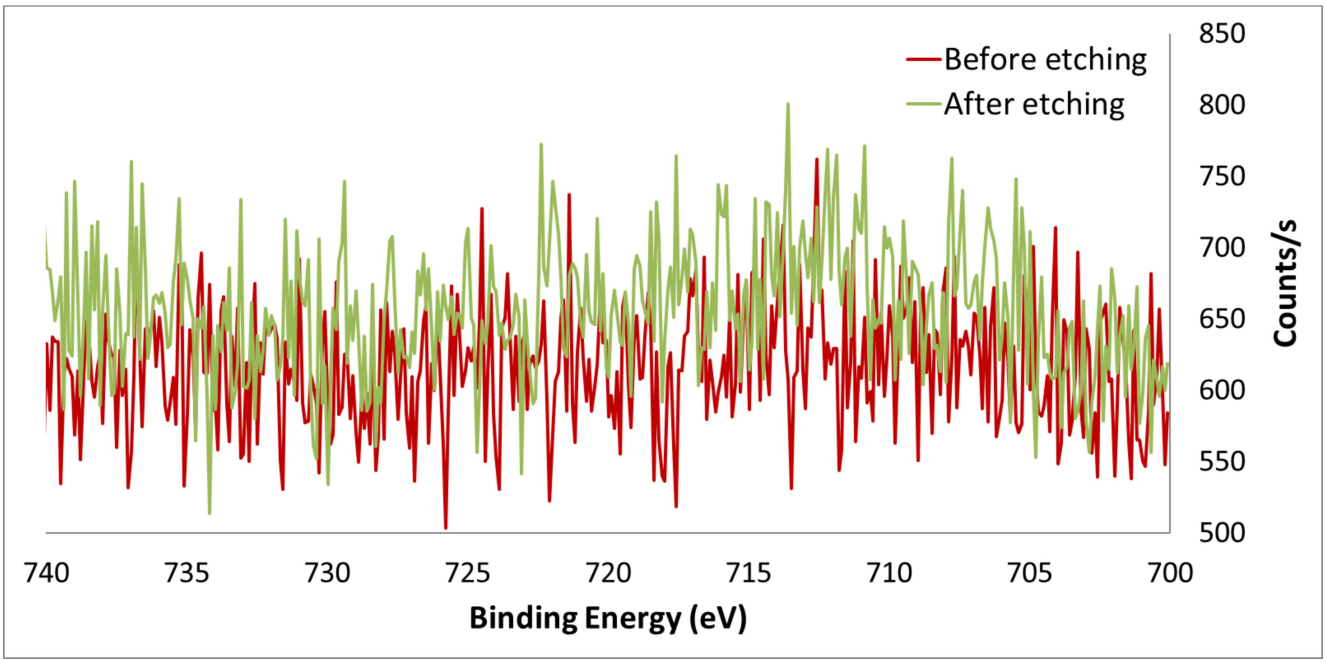

Figure A9. Iron (Fe2p) XPS of the residual oil left on the Ni wire after reaction with Oil A at 200°C before and after etching.

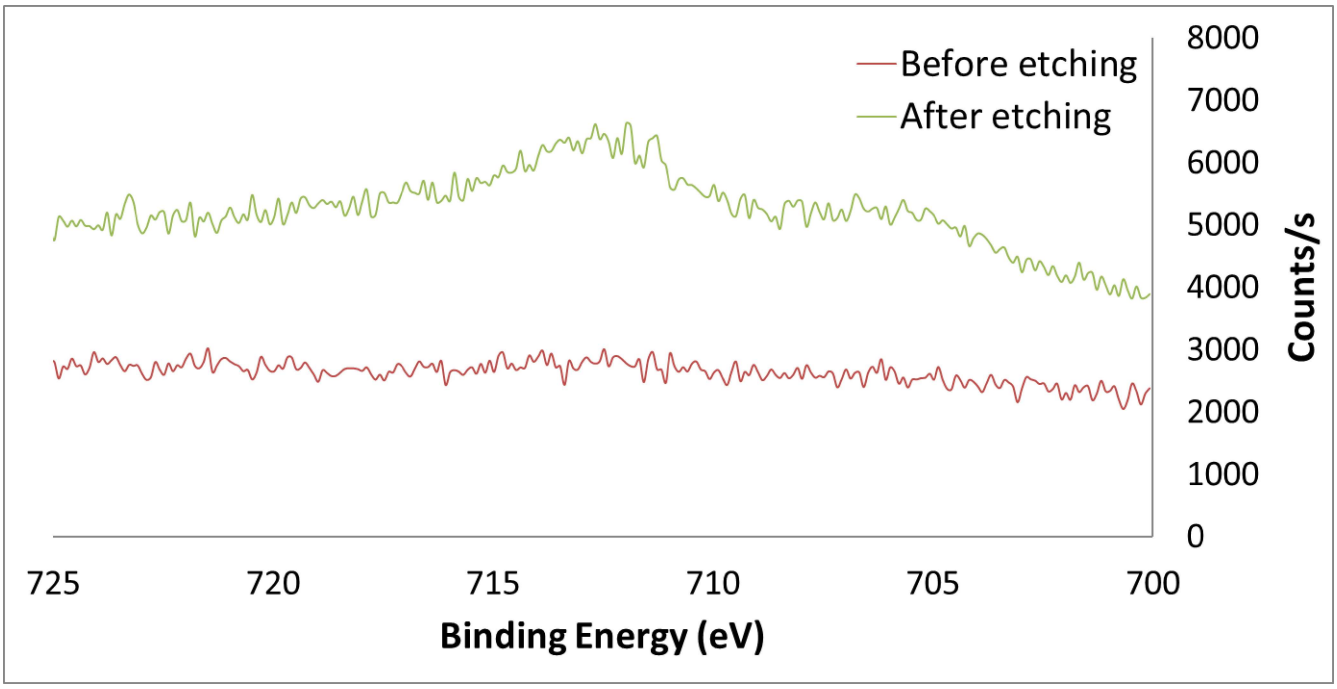

Figure A10. Iron (Fe2p) XPS of the residual oil left on the Ni wire after reaction with Oil B at 150°C before and after etching.

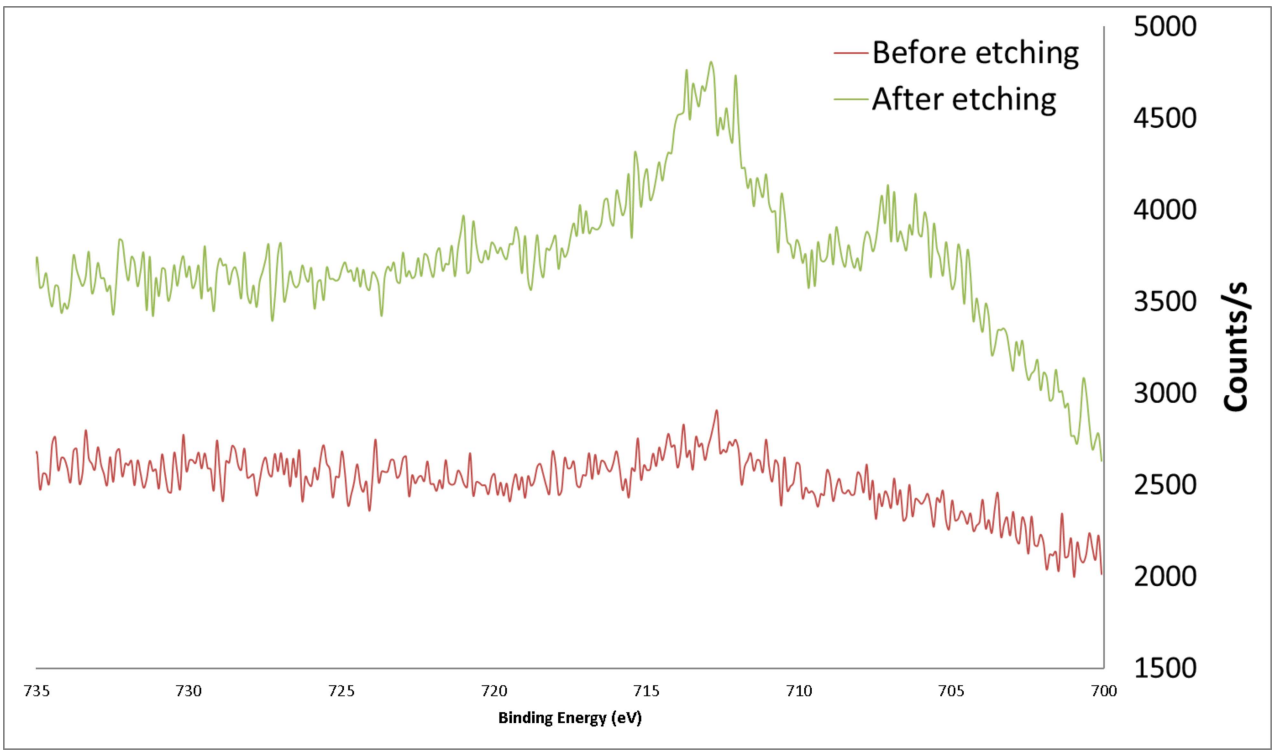

Figure A11. Iron (Fe2p) XPS of the residual oil left on the Ni wire after reaction with Oil B at 200°C before and after etching.

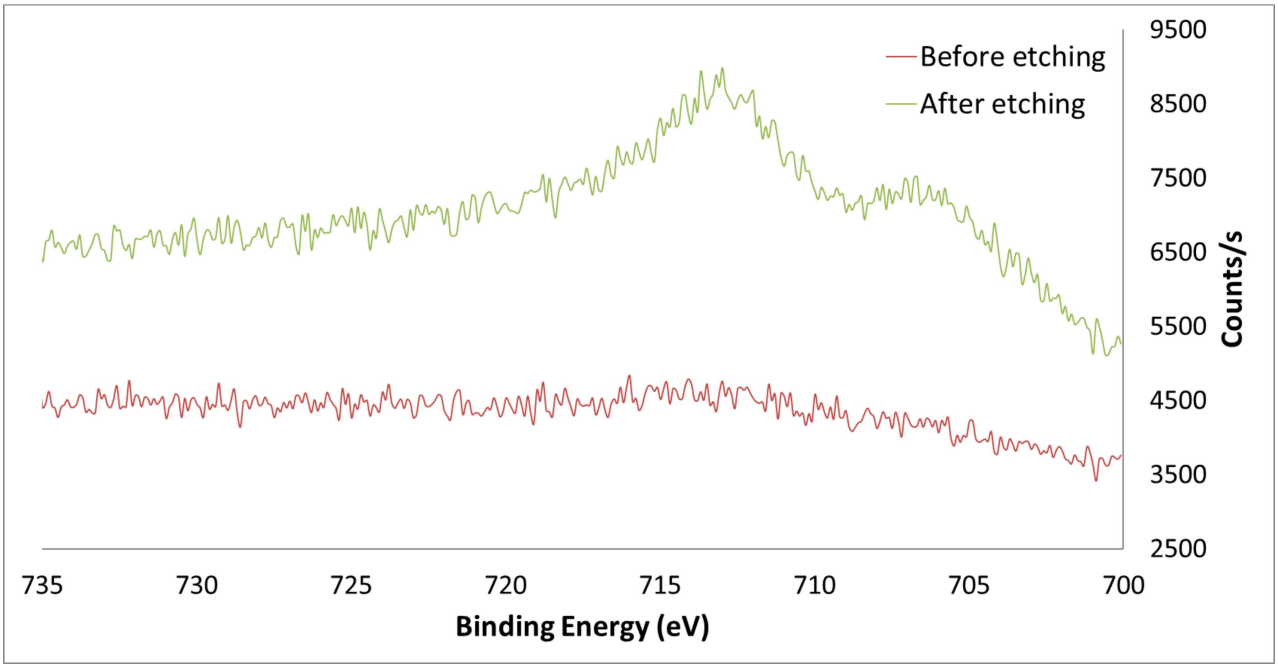

Figure A12. Iron (Fe2p) XPS of the residual oil left on the Ni wire after reaction with Oil C at 150°C before and after etching.

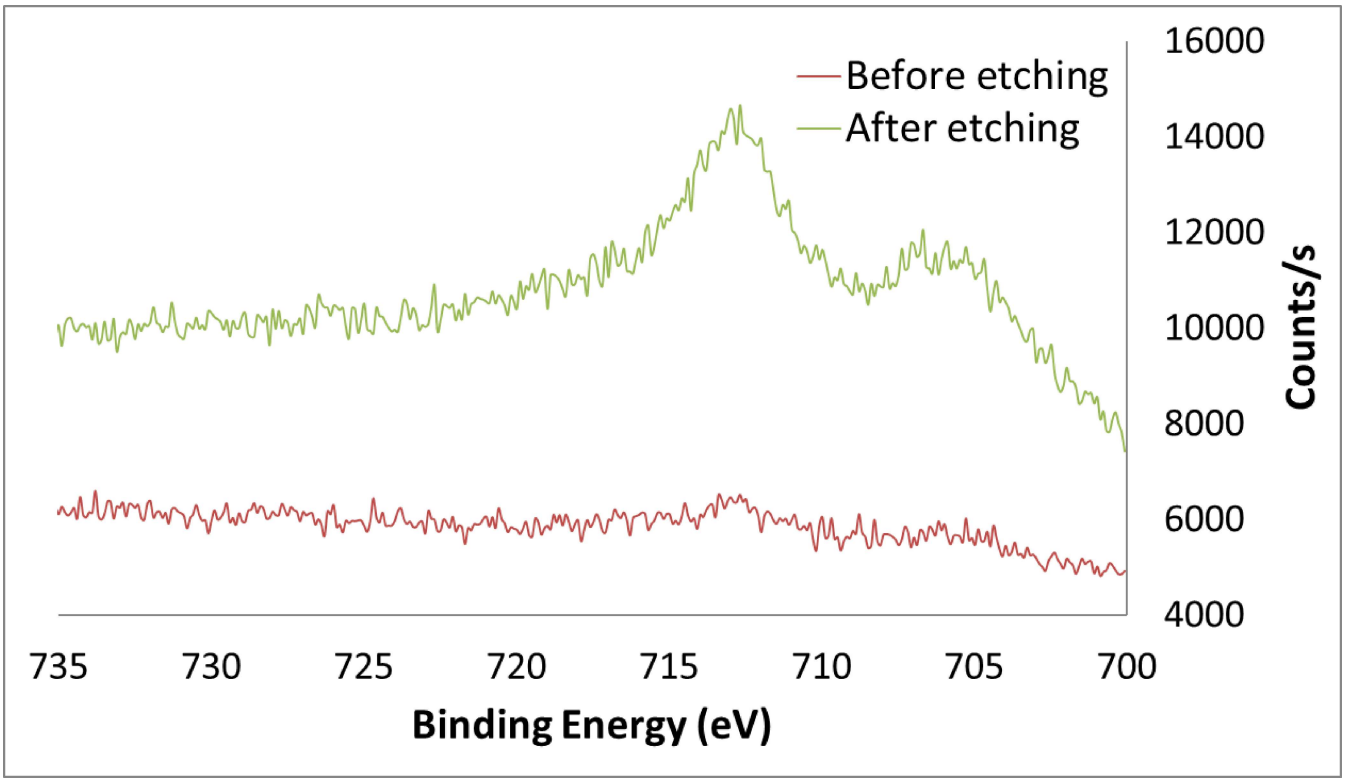

Figure A13. Iron (Fe2p) XPS of the residual oil left on the Ni wire after reaction with Oil C at 200°C before and after etching.

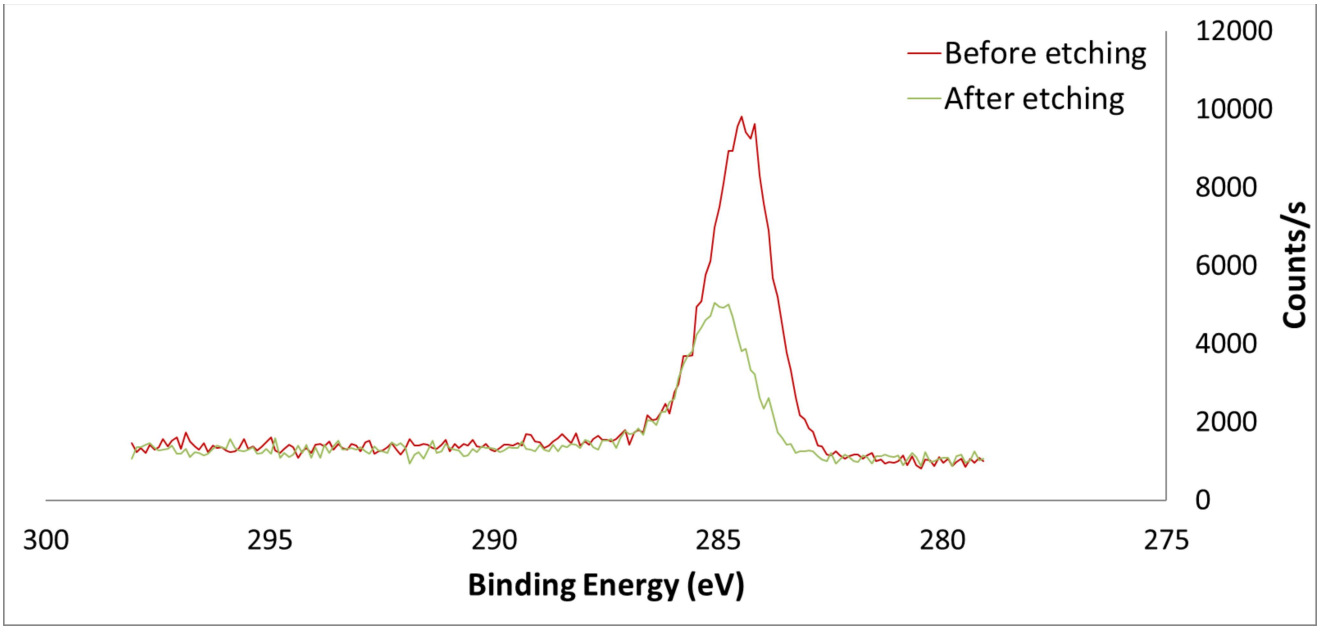

Figure A14. Carbon (C1s) XPS of the residual oil left on the Ni wire after reaction with Oil A at 150°C before and after etching.

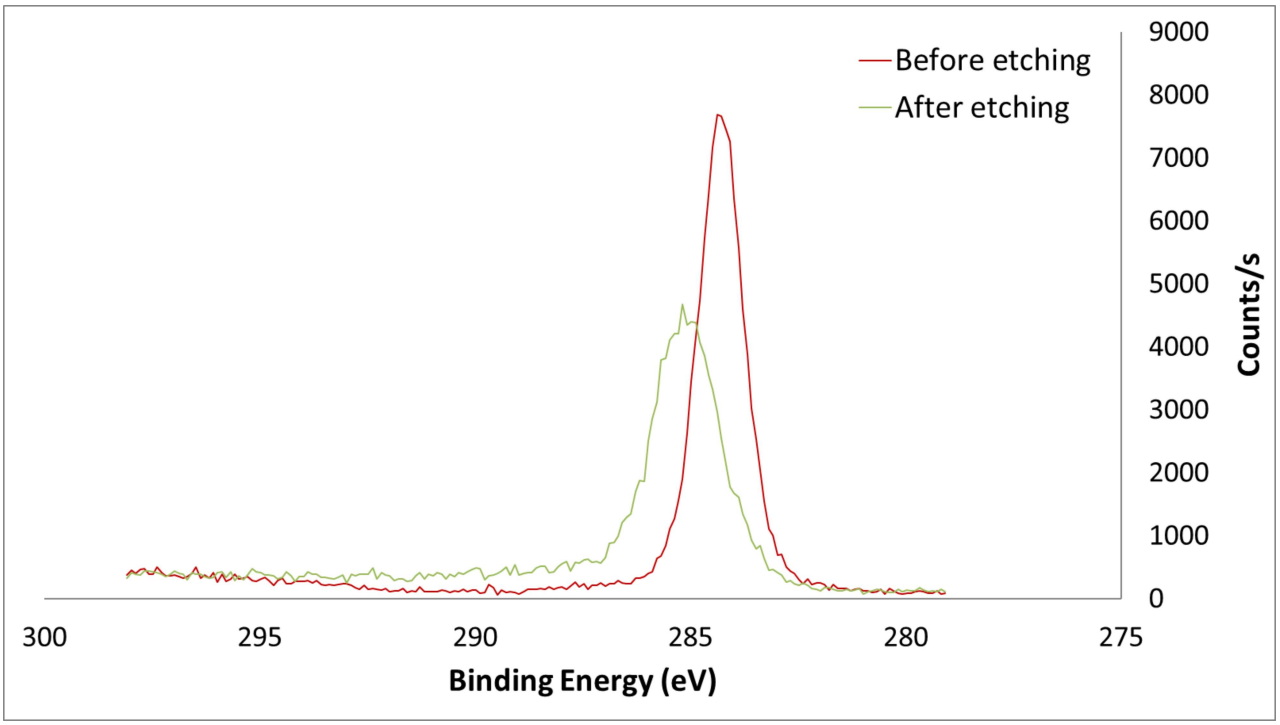

Figure A15. Carbon (C1s) XPS of the residual oil left on the Ni wire after reaction with Oil A at 200°C before and after etching.

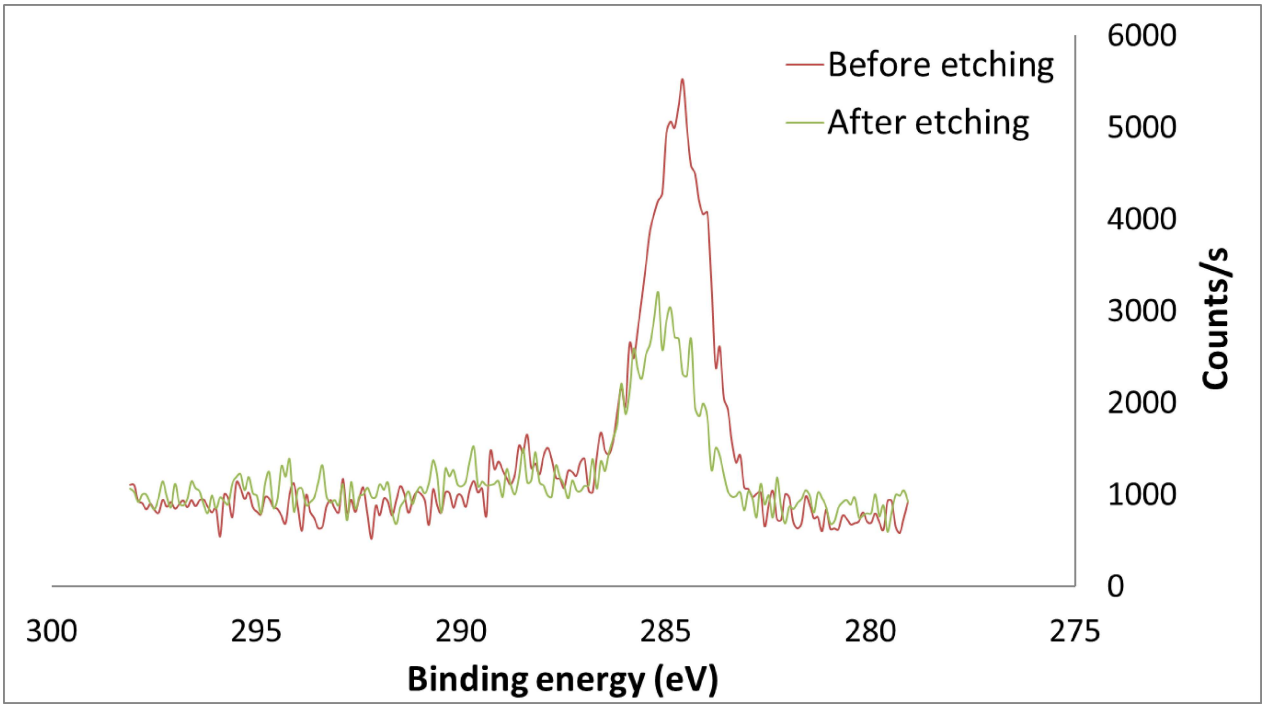

Figure A16. Carbon (C1s) XPS of the residual oil left on the Ni wire after reaction with Oil B at 150°C before and after etching.

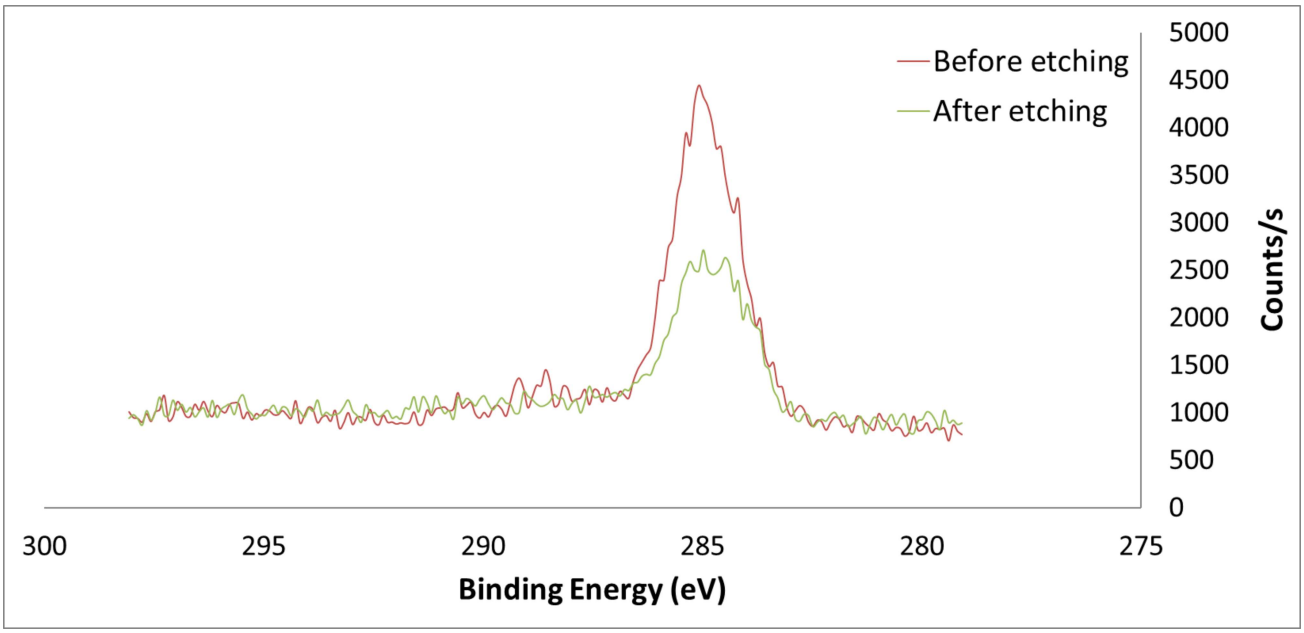

Figure A17. Carbon (C1s) XPS of the residual oil left on the Ni wire after reaction with Oil B at 200°C before and after etching.

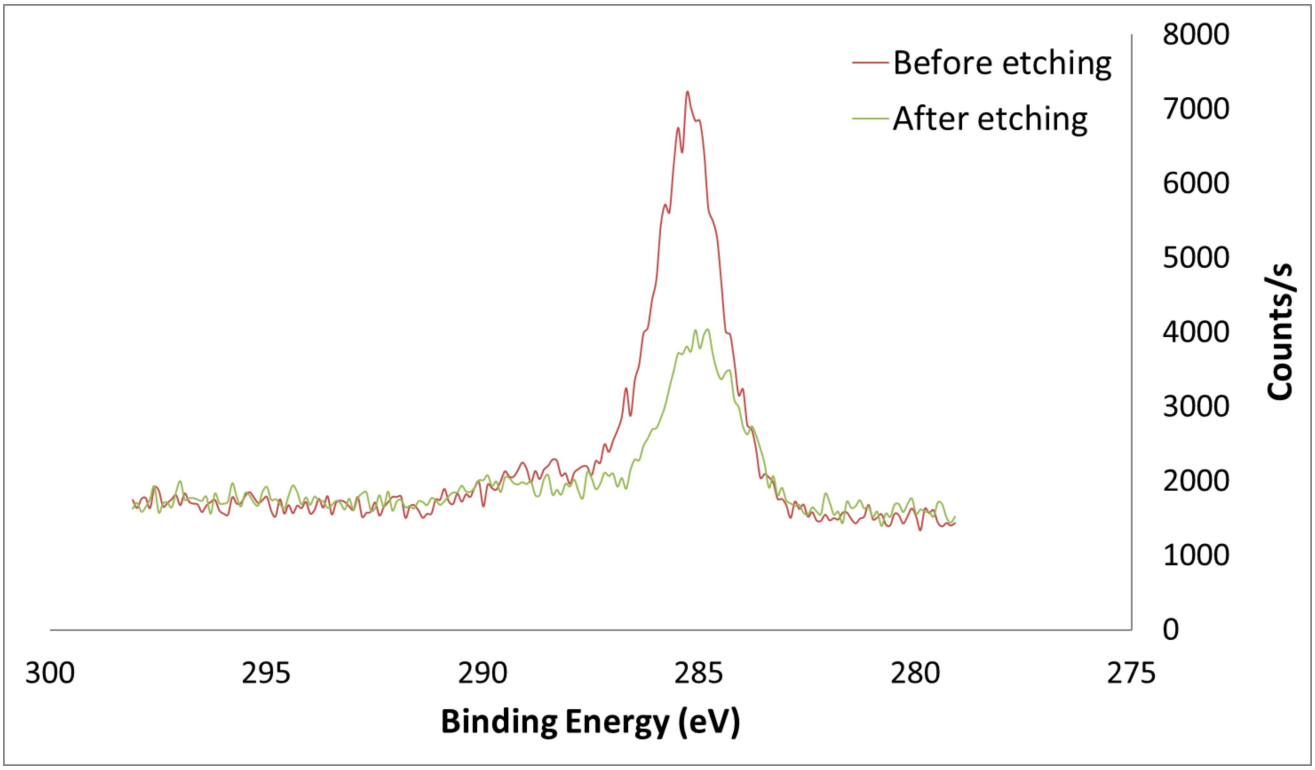

Figure A18. Carbon (C1s) XPS of the residual oil left on the Ni wire after reaction with Oil C at 150°C before and after etching.

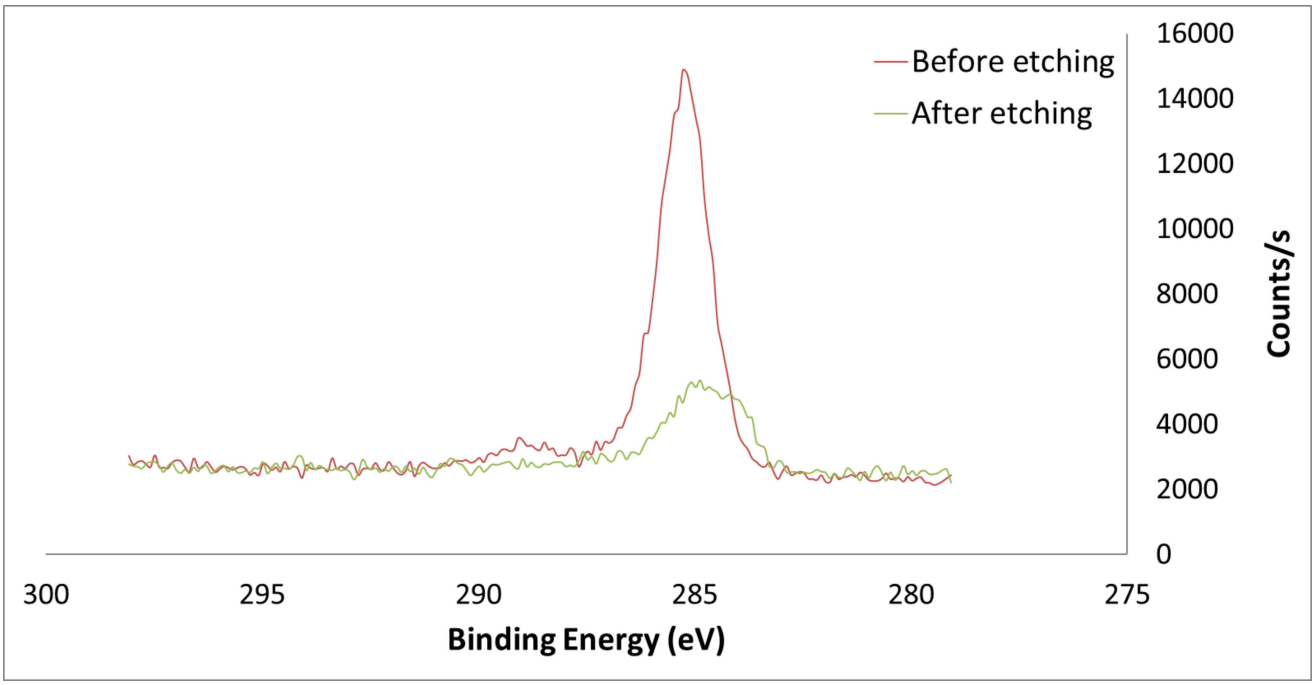

Figure A19. Carbon (C1s) XPS of the residual oil left on the Ni wire after reaction with Oil C at 200°C before and after etching.

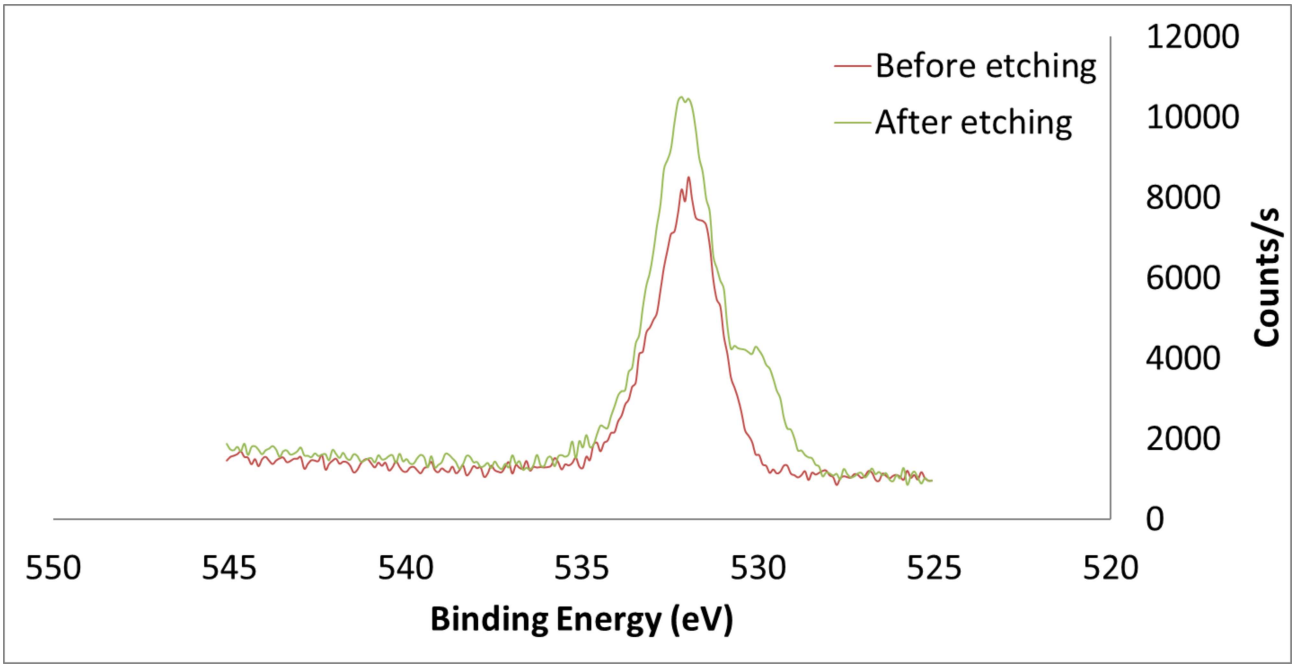

Figure A20. Oxygen (O1s) XPS of the residual oil left on the Ni wire after reaction with Oil A at 150°C before and after etching.

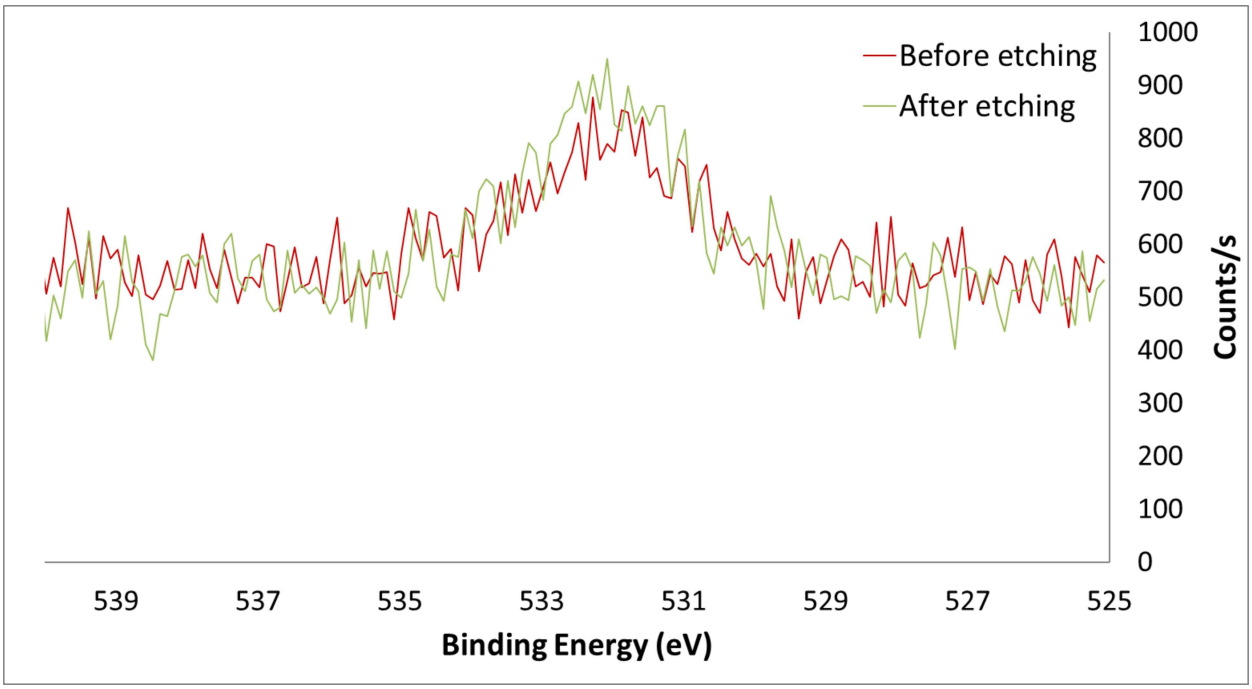

Figure A21. Oxygen (O1s) XPS of the residual oil left on the Ni wire after reaction with Oil A at 200°C before and after etching.

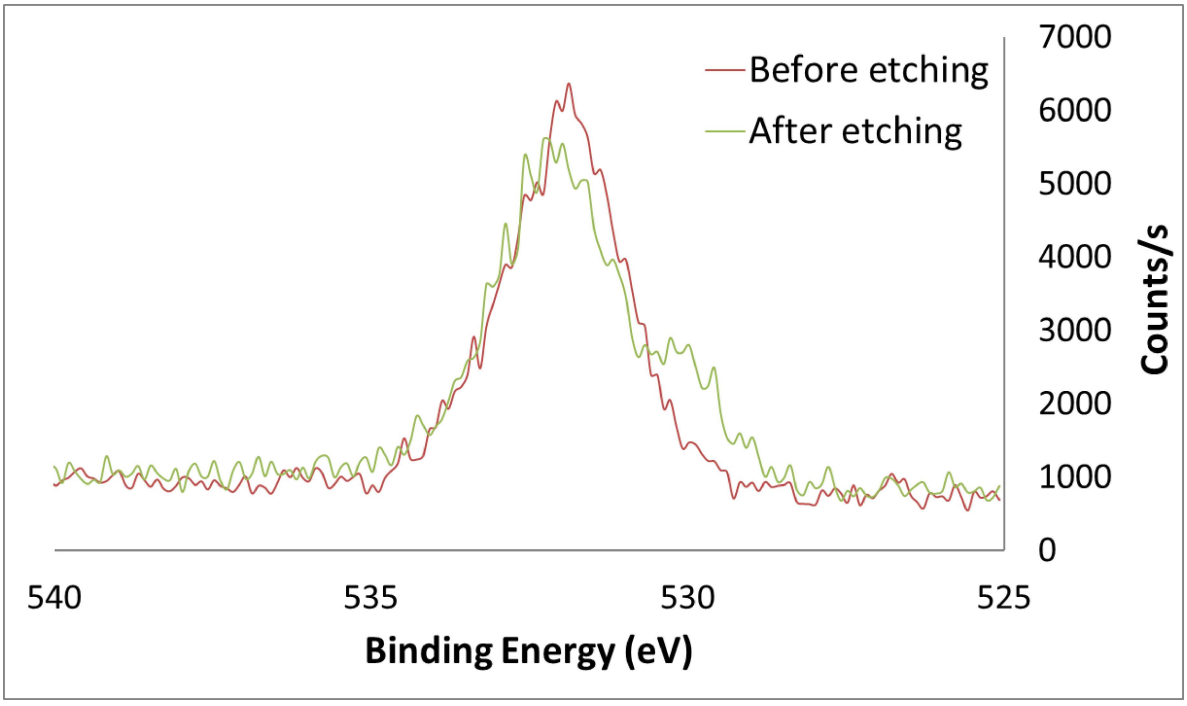

Figure A22. Oxygen (O1s) XPS of the residual oil left on the Ni wire after reaction with Oil B at 150°C before and after etching.

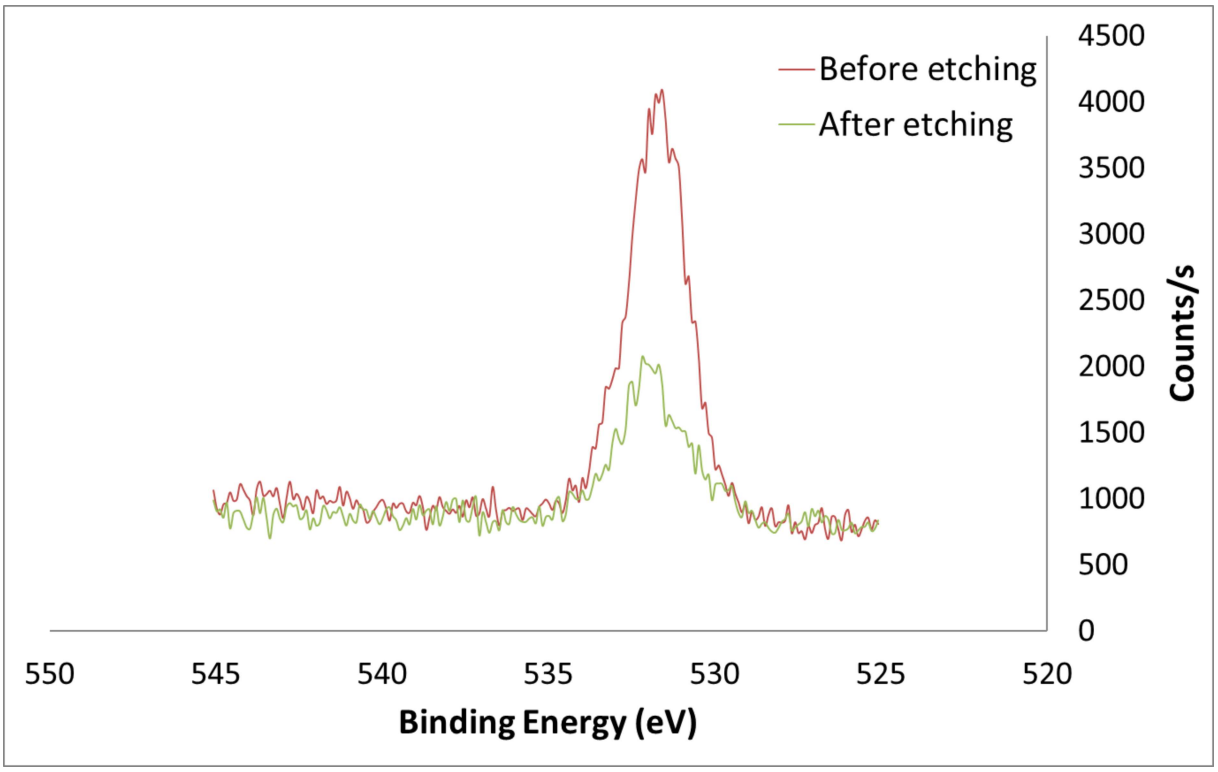

Figure A23. Oxygen (O1s) XPS of the residual oil left on the Ni wire after reaction with Oil B at 200°C before and after etching.

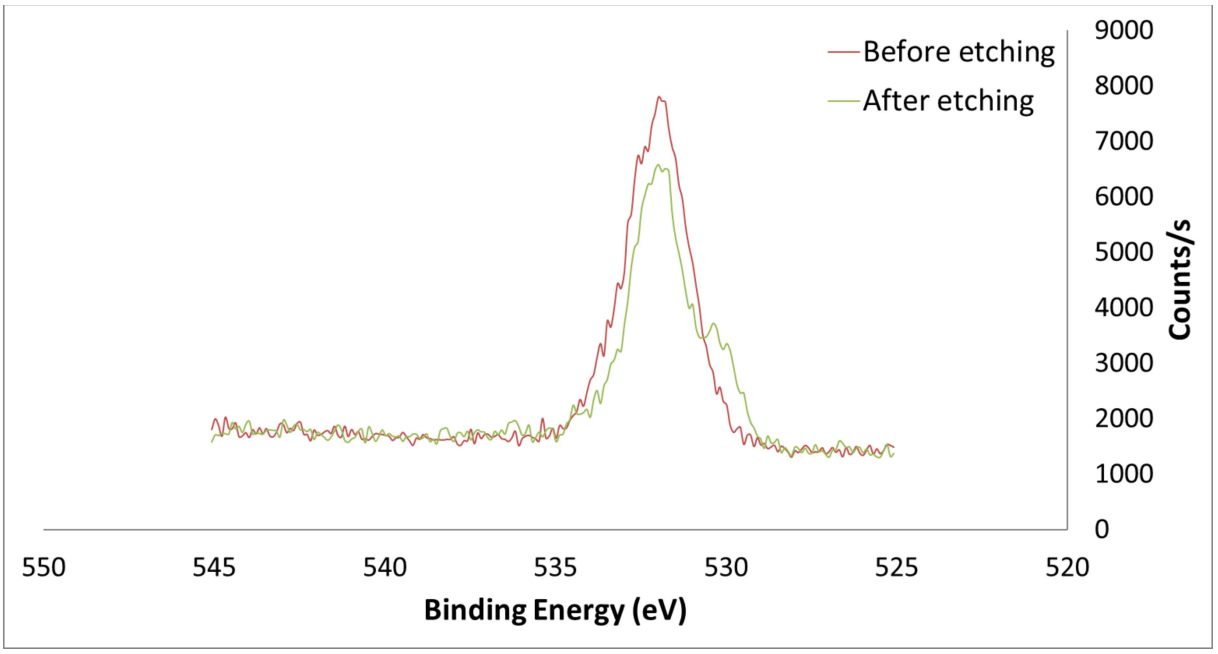

Figure A24. Oxygen (O1s) XPS of the residual oil left on the Ni wire after reaction with Oil C at 150°C before and after etching.

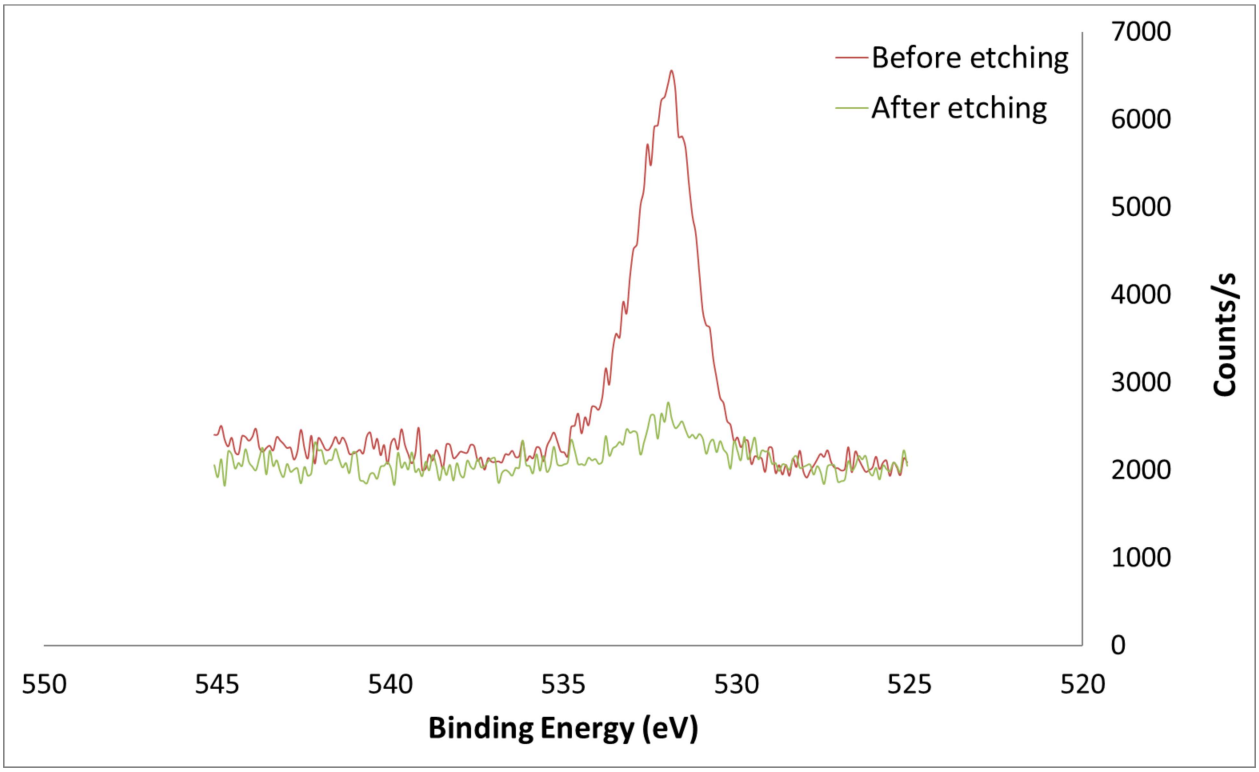

Figure A25. Oxygen (O1s) XPS of the residual oil left on the Ni wire after reaction with Oil C at 200°C before and after etching.

*Declaration of Interest Statement

Sanz-Robinson, J., Williams-Jones, A.E., 2020.
The solubility of Nickel (Ni) in crude oil at 150, 200 and 250 °C
and its application to ore genesis. Chemical Geology, 533: 119443.

Declaration of interests

☒ The authors declare that they have no known competing financial interests or personal relationships that could have appeared to influence the work reported in this paper.

☐The authors declare the following financial interests/personal relationships which may be considered as potential competing interests: